Cranfield University

Manufacturing Systems Department

School of Industrial and Manufacturing Science

MRes Thesis 2005

Written by David Christopher Leeson

PREDICTIVE GRINDING PROCESS OPTIMISATION AND MONITORING.

Supervised by Dr. Tan Jin and Prof. David Stephenson

9th September 2005

(This thesis is submitted in partial fulfilment of the requirements for the Degree of MRes Innovative Manufacturing.)

ABSTRACT

Grinding is one of the oldest and most important metal removal processes, and is capable of high dimensional and surface finish tolerances. It is a complex and expensive process; industry has much to gain by increasing production rates to reduce cost. The major limitation to higher production rates is the risk of thermal damage of the workpiece. This is now being challenged by developments in "High Efficiency Deep Grinding" which has been proven to produce low grinding temperatures at extremely high material removal rates. In order to take advantage of these developments, whilst maintaining the integrity of the workpiece, it is necessary for production engineers to have tools available to them that allow the selection of optimal process parameters and monitor grinding conditions to sustain this optimum.

A review of current research efforts in predictive and reactionary methods of optimising grinding process highlight a number of failings. This study leads to the development of a new system that employs analytical and empirically derived indicators of thermal damage to enable an operator to select optimal but safe grinding conditions. The system also provides a monitoring function that can warn of the onset of thermal damage and make recommendations to the machine operator.

A demonstration of the systems possible benefits in an industrial context is presented. Validation via simulation is also performed. Predicted finished workpiece temperatures are compared against measurements taken using embedded thermocouple and the PVD coating melt depth method. The ability of the system to predict burn is also tested across a range of grinding conditions.

The possibility of using the system as part of an adaptive controller is also reviewed and directions for further work are identified.

ACKNOWLEDGEMENTS

I would like to thank my supervisors Dr. Tan Jin and Prof. David Stephenson for their guidance. Dr. Tan Jin was also kind enough to spend time explaining the complex subject of grinding to me whenever I asked.

Dr. Ian Walton was very helpful, frequently assisting me with error checks on my software and conceptual issues, despite having his own students to supervise.

I would also like to thank my Mother Linda Leeson and Sarah Allen for their support whilst I was writing this thesis.

CONTENTS

FIGURES

TABLES

CHAPTER 1: INTRODUCTION

Grinding is one of the oldest and most important metal removal processes capable of high dimensional and surface finish tolerances. Such is the importance of grinding that Woodbury (1959) even stated that grinding has "...brought profound changes in the way in which we all live." Grinding is also often regarded as the most expensive machining process, Dotto et al (2002). The importance of grinding and its expense means that there is much to gain in increasing the productivity in grinding operations.

Grinding is a very energy intensive machining process and most of the energy expended is converted into heat. This heat energy must be dissipated into the various heat sinks, such as the coolant, grinding wheel and the chip material, if thermal damage of the workpiece is to be avoided. Thermal damage compromises the finished component properties and includes phase transformations, tempering and re-tempering, residual stresses and cracking, Malkin (1989). In steels the tempering and re-tempering is often termed, burn. Rowe (1986) sights the onset of thermal damage to be the greatest obstacle to higher production rates.

The process is also very difficult to optimise as, it is so multivariate and complex that it is generally regarded as something of a black art, Ali (2003). Recent advances in the form of "high efficiency deep grinding", makes the process even more difficult to understand for production engineers. It promises much greater production efficiencies but challenges some of the conventional logic in process design for grinding by suggesting that higher work speeds and larger depths of cut can actually reduce grinding temperatures.

A software tool that can use thermal modelling to enable production engineers to select grinding parameters that lead to the highest production rates without leading to thermal damage has great value in industry and should help dispel some of the confusion surrounding the process. The complexity and transient nature of grinding also means that process monitoring is extremely important, so that inferences about the state of the process maybe drawn and corrective action taken whenever necessary. Such a system could ultimately be integrated into an adaptive control system.

For the purposes of this work the application of these systems shall be limited to steels as this is the most common material ground in industry. Further work should enable them to be modified for additional workpiece materials.

1.1 Aim

The aim of this work is to create a system that is capable of assisting production engineers in process design by selecting conditions that maximise the production rate whilst maintaining the integrity of the workpiece. Furthermore the system should also monitor grinding processes in real time to warn when process conditions approach thermal damage thresholds so that these may be avoided.

CHAPTER 2: LITERATURE REVIEW

This chapter introduces background material necessary for the implementation of the project aims. It begins with a discussion of the general characteristics of different grinding regimes. Following this the development of thermal models for the process are considered along with the thermal effects on surface integrity.

2.1 Grinding

Grinding is one of the oldest and most important metal removal processes capable of high dimensional and surface finish tolerances. Malkin (1989) points out that it is involved in the manufacture of almost all products since grinding is used to produce the tooling for many other manufacturing processes. Such is the importance of grinding that Woodbury (1959) even stated that grinding has "...brought profound changes in the way in which we all live." Grinding is also a very expensive machining process, in fact it is often regarded as the most expensive machining process, Dotto et al (2002). The combination of the importance of grinding and its expense means that there is much to gain in reducing this cost through higher productivity.

Grinding removes material by extremely small and hard abrasive particles, large quantities of these particles are bonded onto a moving substrate to form a grinding wheel, Shaw (1996). These particles interact with the workpiece and remove a large number of extremely small chips. Since the geometry and position of each particle that is involved in these interactions cannot be known, grinding is an extremely difficult process to model and analyse in comparison to conventional metal cutting processes, Malkin (1989). As a result grinding is often considered to be something of a black art where experience rather than physics prevails, Ali (2003).

With any mechanical process there is a release of energy and in grinding virtually all of this energy is converted to heat, Malkin (1989). The heat energy results from elastic and plastic deformation when the grit ploughs through the workpiece. This is exacerbated by wheel wear; flats appear on the grit's cutting face that slide across the workpiece leading to a greatly increased friction component. There is also the energy release from the shearing action along the shear planes of the work material as the

chip is formed. This heat energy has to be dissipated if thermal damage to the workpiece is to be avoided. High grinding temperatures can result in various effects detrimental to the finished workpiece performance: These include phase transformations, tempering and re-tempering, residual stresses and cracking, Malkin (1989). Rowe (1986) also sights thermal damage to the workpiece as the main limitation to material removal rates in grinding. Prudent thermal design of the process is therefore essential in reducing the high cost associated with grinding.

Grinding has traditionally been regarded as a finishing process although this view is being challenged by the development of new grinding regimes. The following four sections summarise the four main regimes of grinding, the later three have been developed to increase the material removal rates possible and therefore reduce cost without loosing the more favourable qualities of grinding. The different geometric arrangements of the work piece such as planar and internal and external cylindrical grinding have not been considered here, as once the obvious kinematic differences have been dealt with these arrangements have identical characteristics.

2.1.1 Conventional Grinding

Conventional grinding uses conservative wheel and workpiece speeds with a shallow depth of cut. It is this conservatism that is the key to avoiding thermal damage to the workpiece in this regime, reducing the energy input into the system. As can be observed from table 2.1 this leads to far lower specific material removal rates (Q'w, which is given by the cut depth ,a multiplied by the workpiece speed, Vw). It is also, chiefly a form and finishing process used to achieve high dimensional and/or surface roughness tolerances on a component that has already undergone one or more other processes. This means that the component may already have significant value added to it when it reaches this stage and so the consequences for a scrapped component are worsened.

2.1.2 Creep Feed Grinding

Creep feed grinding has been common place in industrial since the late 1960's. Malkin (1989), suggests that this process originated from a combination of the

properties of milling and electrolytic grinding. With reference to table 2.1, it can be seen that creep feed grinding is distinguished by slow workpiece speed and very high depths of cut. This type of grinding has wider applications; firstly to finish or form-grinding and secondly as a stock removal process. Careful process design allows an increase in material removal rate without degrading surface roughness or integrity due to thermal effects. Thus creep feed can be more efficient than conventional grinding. This is achieved by increasing the depth of cut but retaining the low workpiece speed to maintain low finished surface temperatures.

2.1.3 High Speed Grinding

At a similar time to the development of creep feed grinding increasing improvement in the construction of grinding wheels allowed much higher wheel speeds to be used. This allowed the evolution of high speed grinding which utilised a small depth of cut with extremely high workpiece speeds. The specific material removal rate is therefore increased over conventional grinding by this high feed rate. It was also found that CBN (Cubic Boron Nitride) wheels and careful application of coolant we're necessary to bring finished workpiece temperatures down to acceptable levels, Gibbons (2005).

2.1.4 High Efficiency Deep Grinding

High efficiency deep grinding or HEDG can be thought of as the combining of the properties of creep feed and high speed grinding: HEDG is characterised by simultaneous increases in wheel speed, depth of cut and work feed-rate thus permitting extremely high stock removal rates as can be observed from table 2.1. Tawakoli (1993) one of the early researchers on the subject performed laboratory trials with material removal rates of up to Q'_w 1000mm^3/mm.s. The total net power was seen to remain approximately constant with increased Q'_w meaning that the energy seen by the workpiece did not increase in proportion with the specific material removal rate. As already stated virtually all this energy is converted to heat and so it follows that the heat input into the work piece should also not have increased. Tawakoli (1993) concluded that the increased workpiece speed meant there was less time for the heat generated to be conducted away from the grinding contact zone and that much of this energy was being removed in the chip material thus keeping the

finished workpiece temperature below critical levels. Based on this principle he suggested that the surface temperature would vary with Q'_w as shown in figure 1.

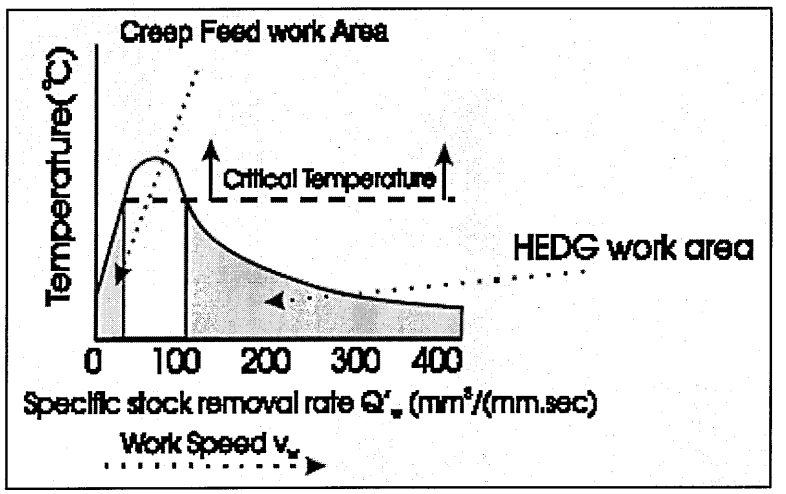

Figure 2.1: Predicted HEDG Curve, Tawakoli (1993).

Further work by Stephenson et al, (2001) found that at high Q'_w values associated with HEDG that around 10% of the heat entered the workpiece. This is also supported by work performed by Rowe (2001b and 2001c) by both thermal modelling and grinding trials.

Machine Parameters	Regime		
	Conventional	Creep Feed	HEDG
Depth of Cut a (mm)	Low 0.001 – 0.05	High 0.1 - 30	High 0.1 - 30
Workpiece Speed V_w (m/min)	High 1 - 30	Low 0.05 – 0.5	High 0.5 - 10
Wheel Speed V_s (m/s)	Low 20 - 60	Low 20 - 60	High 80 - 200
Specific Material Removal Rate Q'_w (mm^3/mm.s)	Low 0.1 - 10	Low 0.1 - 10	High 50 - 2000

Table 2.1: Comparison of Different Grinding Regimes, Tawakoli (1993).

2.2 Grinding Geometry

It is important to have a basic understanding of the geometry of the grinding process in different arrangements so that some basic quantities can be defined that will be used in later analyses.

Figure 2.2 shows the three geometric arrangements that are considered as part of this work, namely planar or surface grinding and internal and external cylindrical grinding.

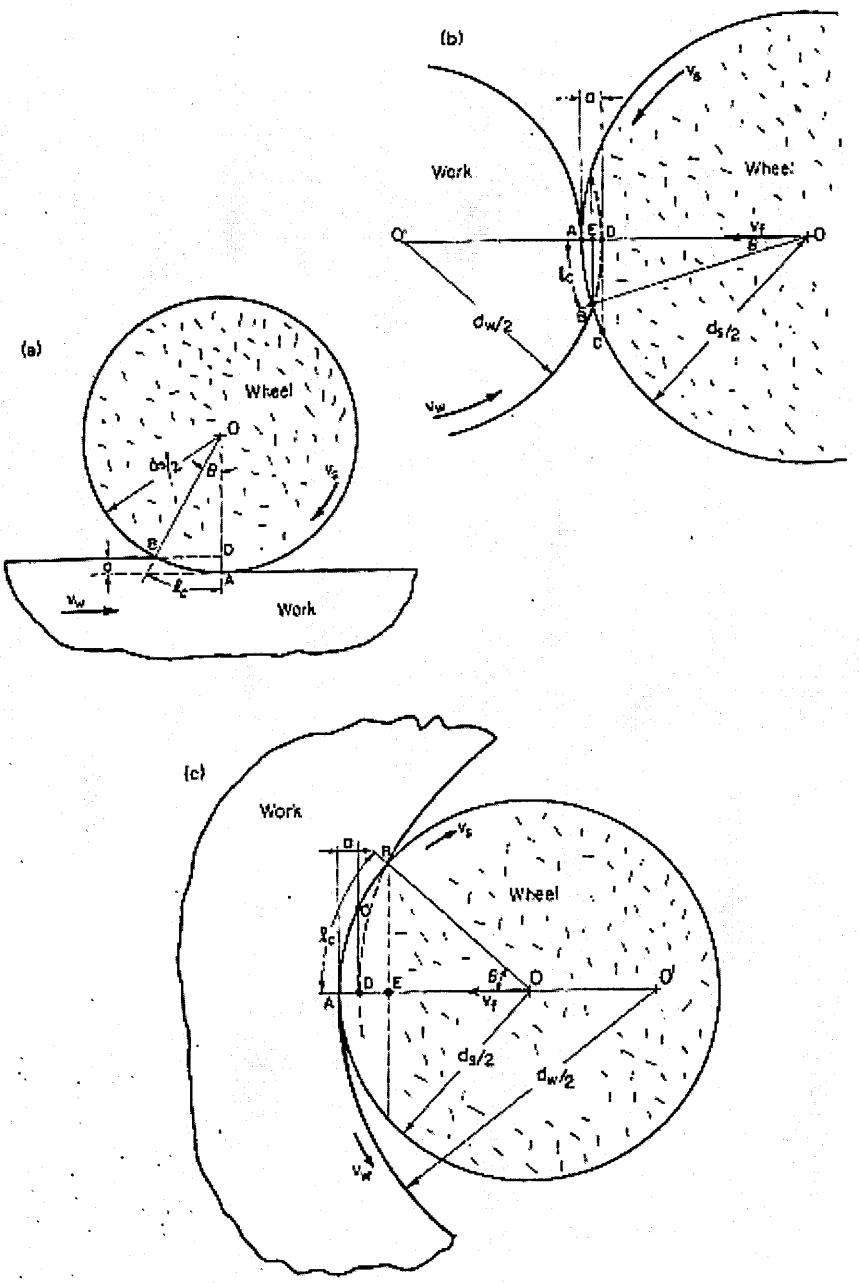

Figure 2.2: Grinding geometry, Malkin (1989)
a) Surface or Planar b)External c)Internal.

Note that in all cases the diagrams show a wheel of diameter d_s rotating at a velocity V_s, penetrating the workpiece by a cut depth a, and translating with a velocity V_w. In cylindrical grinding V_w is calculable from the workpiece rpm and diameter d_w and the depth cut is given by the in feed V_f during one revolution of the workpiece ($a = d_w V_f / V_w$), Malkin (1989).

The interaction of the wheel with the workpiece results in a contact length which is clearly an arc. Since the cut depth is insignificant compared to the wheel diameter the small angle approximation is valid and the contact length l_c is given by:

$$l_c = (a\, d_s)^{1/2} \qquad (2.1)$$

To cover the cylindrical grinding scenarios a quantity called the equivalent wheel diameter d_e is introduced, Malkin (1989) defines this as:

$$l_c = (a\, d_e)^{1/2} \qquad (2.2)$$

Where:

$$d_e \equiv d_s / (1 \pm d_s / d_w) \qquad (2.3)$$

The plus sign is for external grinding, the minus for internal grinding. Clearly, in the case of surface grinding $d_w = \infty$ and so $d_e = d_s$.

2.3 Thermal Modelling in Grinding

Grinding is a very energy intensive process, this energy input results in an elevated workpiece temperature. The exact influence of the grinding energy on the finished workpiece temperature depends on how energy is dissipated into various sinks.

Outwater and Shaw (1952) considered the possible ways in which grinding energy can be removed from the grinding zone:

1) The heat conducted away from the grinding wheel.
2) The heat conducted away by the workpiece.
3) The heat dissipated to the coolant via convection.
4) The heat carried away by the chip material.
5) The kinetic energy imparted to the chips.
6) The energy required to generate a new surface.
7) The residual energy imparted to the ground surface.

Outwater and Shaw (1952) also concluded that the later three sinks are insignificant in comparison to the others, which leads to the logical assumption that all of the grinding energy is converted to heat. This situation is represented pictorially by figure 2.3.

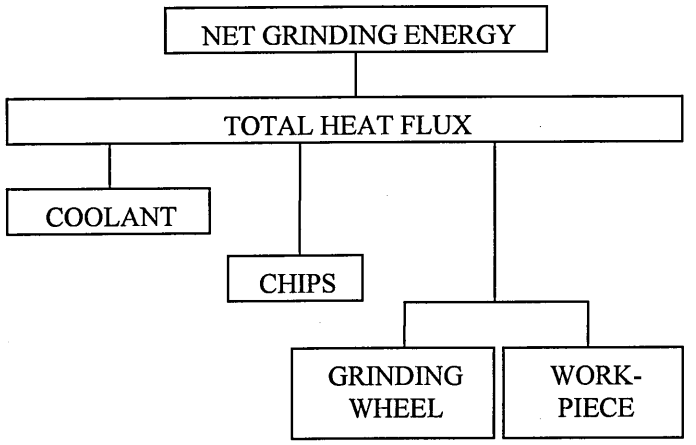

Figure 2.3: Energy Partitioning.

In the following sections a brief historical review of thermal modelling in grinding will be presented followed by a detailed description of the process of calculating finished workpiece temperatures. Particular reference to the derivation of energy partitioning coefficients that determine how the heat flux is dissipated is made.

2.3.1 Historical Review of Thermal Modelling in Grinding

Much work has been performed on the thermal modelling of the grinding process and reviews have been written on these proposed models, notably by Marinescu, I. B. et al (2004).

The first model, upon which many others are based, is that of Jaeger (1942). This model was designed to describe grinding with constant feed rates, light depths of cut. It assumes that the heat source can be represented as flat surface with a uniform heat flux and that the majority of the heat generated by the sliding heat source enters the workpiece. This model provides adequate approximation of grinding temperatures within the bounds of its intended application and is given by the equation 2.3:

$$T_{max} = C \cdot \frac{q_w}{\beta_w} \cdot \sqrt{\frac{l_c}{v_f}} \qquad (2.3)$$

Where:

T_{max}: Maximum Contact temperature in degrees Centigrade.

qw: Heat flux into the Workpiece.

Bw: Mean Thermal Property of Workpiece.

l c Contact length.

v_f: Workpiece Velocity.

C: Constant Dependant on Process Conditions.

However if we are to consider processes with large depths of cut and high material removal rates as is typical for HEDG a more advanced model is required. It has been demonstrated by Rowe (2001 b) that the Jaeger model greatly over estimates the finished workpiece temperature under these conditions.

Rowe (2001 a) proposed a more advanced method involving an inclined heat source with a triangular distribution of heat flux. This takes account of the distance between the contact surface and the finished workpiece surface. A further enhancement was made with a circular arc of contact representing the heat source and the results found to correlate well with measured temperatures from embedded thermocouples, Rowe and Jin (2001 c). The concept of a circular arc heat source can be seen in figure 2.4.

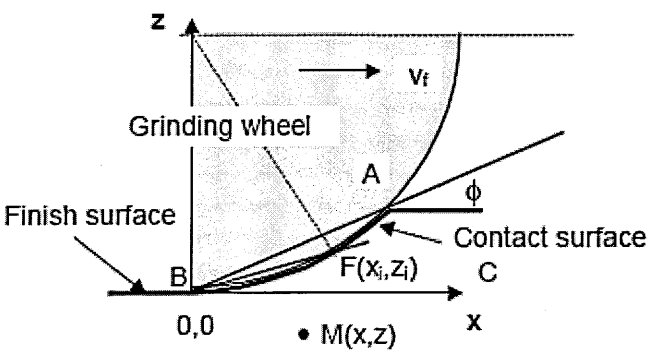

Figure 2.4: The Circular Arc of Contact Heat Source, Rowe and Jin (2001 c).

According to Rowe and Jin (2001 c) the temperature rise at a point M (x, z) in the workpiece due to the whole heat source is:

$$T = \frac{1}{\pi k}\int_0^{lc} q.e^{\frac{v_f(x-l_i\cos\phi_i)}{2\alpha}} K_o\left\{\frac{v_f\left[(x-l_i\cos\phi_i)^2+(z-l_i\cos\phi_i)^2\right]^{1/2}}{2\alpha}\right\}dl_i \qquad (2.4)$$

Where:

T: Calculated temperature in degrees Centigrade.

q: Average heat flux along the length of the contact length.

e: Exponential function.

k: Thermal conductivity of the workpiece.

K_o: Bessel Function of the Second Order Zero.

l i Portion of Total Contact length Analysed.

v_f: Workpiece Velocity.

x: X co-ordinate.

z: Z co-ordinate.

ϕ i: Contact angle.

α: Workpiece thermal diffusivity.

With heat flux q of the form:

$$q = \bar{q}(n+1)(l_i/l_c) \qquad (2.5)$$

Where n=0 for a uniform heat source and n=1 for a triangular heat source. q is the mean heat flux along the total contact arc AFB. Equation 2.4 can be expressed in dimensionless form when using the following expressions:

$$X = \frac{v_f x}{4\alpha} \qquad (2.6)$$

$$Z = \frac{v_f z}{4\alpha} \qquad (2.7)$$

$$L = \frac{v_f l_c}{4\alpha} \qquad (2.8)$$

Such that:

$$\bar{T} = \frac{\pi \cdot k \cdot v_f}{2 \cdot \alpha \cdot \bar{q}} \cdot T \qquad (2.9)$$

Where:

x: X co-ordinate.

z: Z co-ordinate.

L: Peclet Number.

v_f: Workpiece Velocity.

α: Workpiece thermal diffusivity.

lc: Contact length.

(Note: The Peclet Number is a dimensionless parameter used as it enables a large number of situations to be compressed for comparison as stated in Marinescu, I. B. et al (2004).)

2.3.2 The Temperature Estimation Process

In the following sections the process of calculating finished workpiece temperatures will be reviewed, with particular reference to the derivation of energy partitioning coefficient that determine how the heat flux is dissipated.

2.3.3 Total Heat Flux

The total heat flux qt maybe estimated from the net grinding power or the specific grinding energy (SGE).

The net grinding power is the power required for the machining process neglecting that required to overcome the friction in the machine tool and the hydrodynamic force generated from the coolant in the grinding zone, often known as the "spark out" power. According to Marinescu, I. B. et al (2004) "...the rate of heat generation is

almost exactly equal to the rate of heat generation in the abrasive contact zone." Hence the total heat flux qt is given by:

$$q_t = P_{net} / l_c \,.\, b \qquad (2.10)$$

Where:

P_{net}: Net grinding power.

lc: Contact length.

b : Grinding width.

The net grinding power cannot be accurately predicted for a given process and so equation 2.10 is only suitable when the grinding power can be monitored.

Stephenson and Jin (2003) have proposed expression to estimate the SGE for a given type of grinding condition and coolant supply strategy:

$$e_c = A \,.\, Q'w^{-t} \qquad (2.11)$$

Where e_c is the SGE in J/mm^3, Q'w is the specific material removal rate in $mm^3/mm.s$ and A and t are constants that depend on the workpiece material and grinding conditions, examples of which can be seen in table 2.2. The specific material removal rate is given by:

$$Q'w = a \,.\, v_w \qquad (2.12)$$

Where:

a: Cut depth.

v_w: Workpiece velocity.

Workpiece/Abrasive	A	t	v_s (m/s)
Steel/CBN	70	0.25-0.4	100 ~ 150
Steel/ Al_2O_3	140	0.45	60
IN718/CBN	150	0.28	150
MAR M002/CBN	400	0.7	150
Ti-6-4/Al_2O_3 (shallow cut)	106	0.56	30
Ti-6-4/Diamond (shallow cut)	53.1	0.0619	30

Table 2.2: Values for the parameters A and t, Stephenson and Jin (2003)

Equation 2.11 is derived from experimental data; a comparison with experimental data can be seen in figure 2.5.

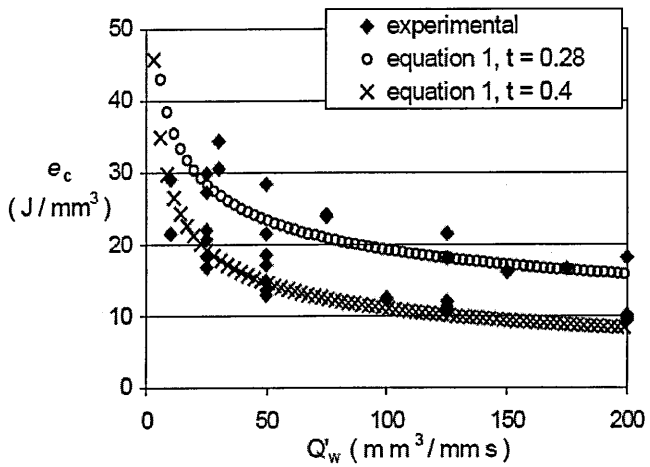

Figure 2.5: Change in Specific Grinding Energy with Specific Material Removal Rate for Surface Grinding of Steel with a CBN wheel.

Stephenson and Jin (2003) indicate that the total heat flux can be evaluated using the SGE from the following expression:

$$q_t = e_c \cdot a \cdot v_w / l_c \qquad (2.13)$$

Thus it can be seen that the total heat flux can be both predicted from an empirically derived relationship and monitored in real time from the grinding power.

According to Rowe and Jin (2001 c), and also implied by figure 2.3, the total heat flux can also be expressed as:

$$q_t = q_w + q_s + q_{ch} + q_f \qquad (2.14)$$

Where:

q_w : Heat flux to the workpiece.

q_s : Heat flux to the wheel.

q_{ch}: Heat flux to the chips.

q_f: Heat flux to the fluid.

These are related to the maximum contact temperature T_{max}, the fluid burn out temperature T_b and the chip temperature T_{ch}. These relationships (shown below) assist in determining the convection factors and ultimately the finished workpiece temperature.

$$q_w = h_w \cdot T_{\max}, \qquad q_s = h_s \cdot T_{\max}$$
$$q_f = h_f \cdot T_{\max}\big|_{T_{\max} \le T_b}, \quad q_{ch} = h_{ch} \cdot T_{ch} \qquad (2.15)$$

Where:

h_w : Convection factor to the workpiece.

h_s : Convection factor to the wheel.

h_{ch}: Convection factor to the chips.

h_f: Convection factor to the fluid.

The expressions for the individual convection factors can now be derived.

2.3.4 Convection Factor to the Grinding Wheel

According to Rowe and Jin (2001 c) a convection factor for the abrasive grains of the grinding wheel can be estimated using the Hahn model of a grain sliding on the workpiece surface, Hahn (1962). This gives the ratio of the heat flux divided between

the workpiece and the wheel. It is generally termed the "workpiece-wheel partition ratio" and is given by equation 2.16:

$$R_{ws} = \frac{q_w}{q_{ws}} = \frac{q_w}{q_w + q_s} = \frac{h_w}{h_w + h_s} = \left[1 + \frac{0.97 k_g}{\beta_w \sqrt{r_o v_s}}\right] \qquad (2.16)$$

Where:

k_g: Thermal Conductivity of grains.

β_w: Mean Thermal Property for Workpiece.

r_o: Effective Radius of contact of a grain.

v_s: Wheel Speed.

and:

$\beta_w = \sqrt{k \,.\, \rho \,.\, c}$ (Mean Thermal Property) (2.17)

k: Wheel conductivity.

ρ: Wheel Density.

c: Wheel specific Heat Capacity.

β_w is Thermal properties of materials such as specific heat capacity and are temperature dependant although the property of concern β_w is much less sensitive. As Malkin (1989) indicates this is partially because the increase in specific heat capacity partially offsets the effect of the decrease in conductivity and so taking a mean value is a valid approach. Malkin (1989) also suggests that taking an iteratively calculated value for the thermal property based on the grinding zone temperature is questionable since the temperature gradients are so steep. Experimental work by Walton (2005) supports this view.

Rowe and Jin (2001 c) suggests that the value of r_o is not highly sensitive and a value of 10 microns is taken to indicate a relatively sharp wheel. Later work by Stephenson (2001) suggested that the radius should vary linearly with usage from 4 to 15 microns since "...the grit wear flat follows a classical Archard wear relationship".

Thus the ratio of heat flux to the workpiece and wheel can be determined.

2.3.5 Convection Factor to the Grinding Fluid

Rowe et al. suggested convection coefficients (h_f) for water and oil of 23000W/m^{2}K and 290000 W/m^{2}K, respectively. This is much higher than previously estimated although much experimental work by Rowe, Jin and Stephenson has verified these values.

Jin, Stephenson, Rowe, (2003) also estimated the fluid convection factor with hydrodynamic modelling of the grinding zone. It was found that the convection factor increases with wheel speed due to the agitation of the fluid (this was also noted by Malkin 1989) and the fluid film thickness. This can be observed in figure 2.6.

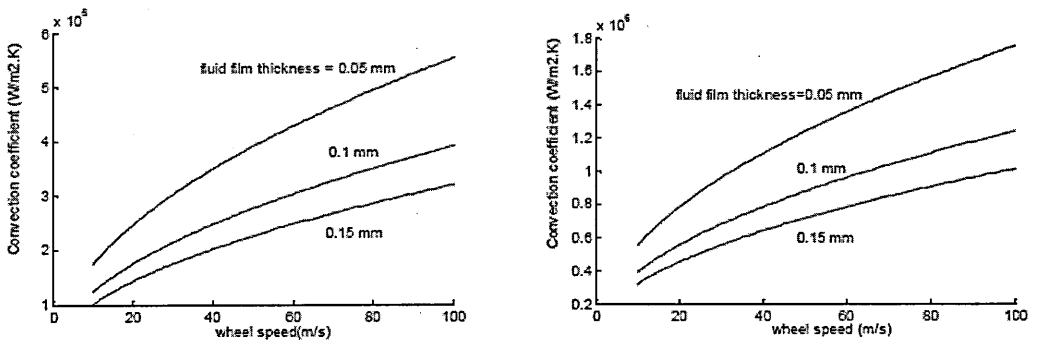

(a)neat oil at room temperature (b)water at room temperature

Figure 2.6: Variation in Fluid Convection Factors with Film Thickness and Wheel Speed, Jin, Stephenson, Rowe, (2003).

Clearly calculating the convection coefficients in this way requires knowledge of the film thickness which is not a simply obtainable parameter.

A very important effect to consider is the effect of the transition from nucleate to film boiling. Malkin (1989) states that during nucleate boiling "...bubbles nucleated at the surface agitate the fluid and promote cooling..." and conversely, in film boiling "... a continuous vapour insulates the heated surface and hinders cooling." After this transition the cooling effect of the fluid is greatly reduced, Rowe and Jin (2001 c) declare that in this state the coolant makes no significant contribution to cooling and so $h_f = 0$. Furthermore this transition occurs at a distinct threshold related to the mean contact temperature, T_{mean}. Malkin (1989) states the transition temperatures (t_b) for

steels with water and oil based fluids, which are 130°C and 300°C respectively. Rowe and Jin (2001 c) also indicate that T_{mean} is equal to approximately $0.67T_{max}$ and so the transition temperatures have to be adjusted to suit.

2.3.6 Convection Factor to the Grinding Chips

There are three possible approaches described in the literature that determine the amount of energy partitioned to the chips.

Intuitively, the heat flux to the chips is given by the product of the energy contained in a unit volume of the chip material and the specific material removal rate, divided by the contact length. The contact length being the surface from which heat is generated. This leads us to the following equation, Rowe and Jin (2001 c):

$$q_{ch} = e_{ch} \cdot a \cdot v_f / l_c \qquad (2.17)$$

Where:

e_{ch} : Energy within Chip.

a: Depth of Cut.

vw : Feed Rate.

lc : Contact Length.

and:

$$e_{ch} = \rho \cdot c \cdot T_{ch} \qquad (2.18)$$

ρ: Workpiece Material Density.

c: Workpiece Specific Heat Capacity.

T_{ch}: Chip Temperature.

Hence:

$$h_{ch} = \rho \cdot c \cdot a \cdot v_f / l_c \qquad (2.19)$$

h_{ch}: Convection Factor to Chips.

Outwater (1952) demonstrated that the chip shear plane temperature can exceed 1000°C for gentle conditions and even approach the melting temperature of the material. Rowe and Jin (2001 c) took the chip temperature to be 1500°C assuming that under HEDG conditions the chips would approach the melting point, this results in a limiting chip energy of 8.1 (J/mm^3) for steel. Clearly this chip energy will change with the temperature dependence of specific heat capacity; there is some debate whether to use a value appropriate to the estimated chip temperature as is described in an unpublished paper by Jin and Stephenson that has been submitted to the IMechE.

Later work by Jin and Stephenson (2001), considered the variation in the chip temperature with process conditions. They point out the difficulty in accurately estimating the chip temperature since it is related to such things as the chip shear angle and length and the grain wear flat area for each individual grain. It was proposed that the chip temperature could be approximated by assuming the chip temperature varies linearly between 1000°C and 1500°C with the maximum workpiece surface temperature since this is also ultimately determined by these process conditions. Hence:

$$T_{ch} = 1000 + T_{\max} / 3 \qquad (2.20)$$

The heat flux to the chips can then be evaluated using equations 2.17 and 2.18. The use of this method requires an iterative calculation to be performed since T_{ch} and T_{max} are co-dependent. It is also suggested in the same paper, that the same linear assumption should be made for the variation of specific heat capacity, in order to select a value appropriate to the estimated chip temperature.

Work by Jin and Stephenson (2005 a) that has been submitted to the IMechE for publishing, proposes an alternative approach, where a sub analysis of the heat partitioning on chip formation is performed. This method allows the variation in chip energy with specific material removal rate to be calculated. According to Loewen and Shaw (1954), the heat partitioning ratio can be given as:

$$R_1 = \frac{1}{1+1.328\sqrt{\frac{\alpha_w \cdot \gamma}{v_s \cdot t_a}}} \qquad (2.21)$$

Where α_w is the thermal diffusivity of the workpiece, v_s is the wheel speed, t_a is the average chip thickness and γ is the shear strain which can be evaluated from equation 2.22:

$$\gamma = \frac{\cos\theta}{\sin\varphi\cos(\phi+\theta)} \qquad (2.22)$$

Where φ is the shear angle and θ is the angle at the chip-rake interface. A sensitivity analysis was performed by Jin and Stephenson demonstrated that φ could be approximated by $\varphi = (90 - \theta)/2$.

The three following equations first put forward by Outwater and Shaw (1952) allow the average chip thickness to be evaluated:

$$t = \left(\frac{4 \cdot v_w}{v_s} \cdot \sqrt{\frac{a_e}{d_s}} \cdot \frac{1}{N_d \cdot r}\right)^{\frac{1}{2}} \qquad N_d = A_g \cdot c_1^{\beta}\left(\frac{v_w}{v_s} \cdot \sqrt{\frac{a_e}{d_s}}\right)^{\alpha} \qquad t_a = \frac{t}{2} \qquad (2.23)$$

Where:

v_w: Workpiece Speed.

v_s: Wheel Speed.

a: Depth of Cut.

d_s: Wheel Diameter.

N_d: Number of Active Grains per Unit Area.

r: Ratio of chip width to thickness, $r = 4 \cdot \tan\theta$.

A_g: Proportional Constant ≈ 1.2

c_1: Static grain density 10~11/mm^2

β: Parameter Relating to the Grain Sharpness and Radial Distribution.

α: Parameter Relating to the Grain Sharpness and Radial Distribution.

t: Maximum Chip Thickness.

t_a: Average Chip Thickness..

The heat partitions are then given as:

$$R_{wch} = 1 - R_1 \quad \text{and}$$

$$R_{wch} = \frac{h_w}{h_{ch} + h_w} \tag{2.24}$$

Where R_{wch} is the heat flux ratio between the workpiece and the grinding chips. Thus convection factor to the chips can be estimated. Jin and Stephenson used this model to show the variation in the fraction of the total heat flux partitioned to the chip (R_{ch}) with specific material removal rate as shown in figure 2.7.

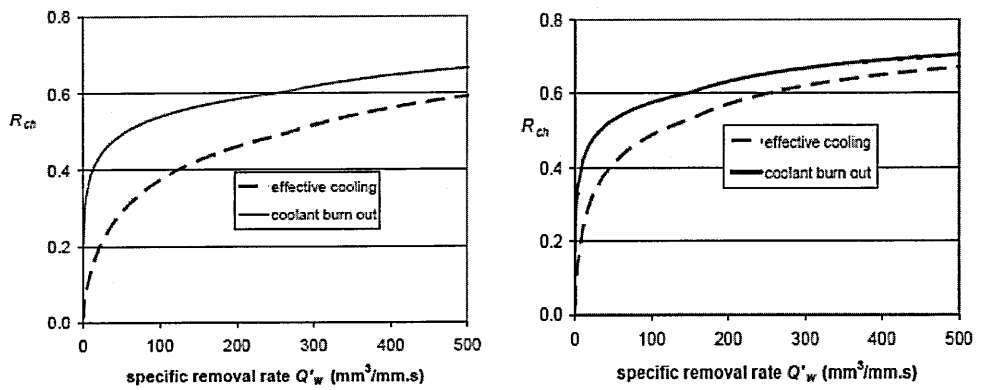

Figure 2.7: Variation in Energy Partition with Specific Material Removal Rate.

Thus the convection factor to the chips can be determined using one of the three methods detailed here.

2.3.7 Convection Factor to the Workpiece

Rowe and Jin (2001) used the Jaeger model, shown in equation 2.3, to create the following expression for the convection factor to the workpiece, (h_w):

$$h_w = \frac{\beta_w}{C} \cdot \sqrt{\frac{v_f}{l_c}} \tag{2.25}$$

The C factor, as it is often referred to, is dependant on contact angle ($\sin\Phi = a / l_c$) and peclet number (equation 2.9), this relationship can be seen in figure 2.8. The other parameters have been explained elsewhere.

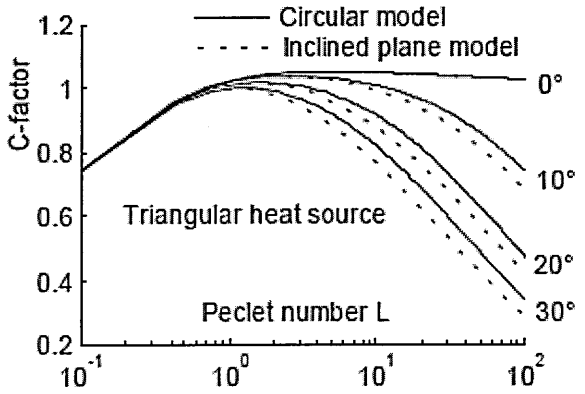

Figure 2.8: Variation in C Factor with Peclet Number and Contact Angle, Rowe and Jin (2001).

2.3.7 Calculation of Temperatures

From the relationships shown in equation 2.15 it is clear that the maximum contact temperature can be estimated from (Rowe and Jin 2001)):

$$T_{max} = \frac{q_t - h_{ch} \cdot T_{ch}}{\frac{H_w + h_f}{R_{ws}}} \quad T_{max} \le T_b \qquad T_{max} = \frac{q_t - h_{ch} \cdot T_{ch}}{\frac{H_w}{R_{ws}}} \quad T_{max} \ge T_b \tag{2.26}$$

Notice the conditional use of the fluid convection factor to take account of the transition from nucleate to film boiling.

The maximum finished workpiece temperature is then required since this temperature determines whether the workpiece has been subjected to thermal damage and hence the mechanical properties of the workpiece. Rowe and Jin found the fraction of contact to finished workpiece temperature to vary with contact angle and peclet number as with the C factor. A graph of this relationship is shown in figure 2.9:

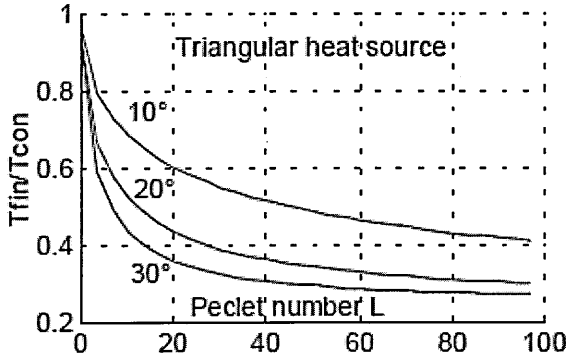

Figure 2.9: Variation in the ratio of Finished Workpiece Temperature and Contact Temperature with Peclet Number and Contact Angle.

Hence from this and the previous sections the finished workpiece temperature can be estimated from monitored power or the ideal specific energy for a given set of process parameters.

2.4 Thermal Damage

As has already been stated, the input of thermal energy during grinding of a workpiece can cause damage that compromises the mechanical properties of the finished component. Field and Kahles (1971) demonstrated that the fatigue life for a ground component could be reduced from 70 x 10^7 to 62 x 10^7 cycles when it is ground abusively (i.e. it is ground with parameters that lead to thermal damage of the workpiece) The following sections provide a summary of the different types of thermal damage that may occur during grinding.

2.4.1 Residual Stresses

Residual stresses are an inevitable part of metal removal by grinding. These are created by non uniform plastic deformation of the workpiece surface, Field and Kahles (1971).

Mechanically induced residual stresses in grinding have a positive effect on the workpiece properties. The interactions of the abrasive grains with the workpiece

produce deformation at the surface and therefore compressive stresses rather like the shot peening process, Malkin (1989).

Residual tensile stresses, on the other hand, are thermal in origin and so are more relevant to this study. When the temperature of the workpiece is raised by grinding there is a temperature gradient between the workpiece surface and it's bulk. The expansion of the hot surface material is restricted by the cooler material underneath and could cause plastic flow in compression should the temperature gradient be high enough. When the workpiece is left to return to ambient temperature the plastically deformed material contracts more than the other material, in order for equilibrium to be maintained tensile stresses are then created at the surface. These tensile stresses have a negative effect on material properties. With high strength materials the tensile stresses may be high enough to produce cracking with a dramatic effect on fatigue life, Malkin (1989).

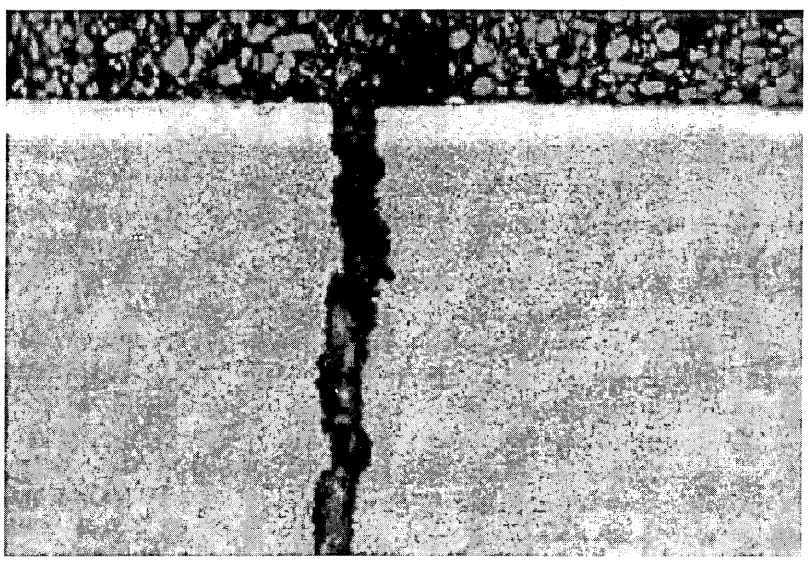

Figure 2.10: Example Surface Cracking due to Abusive Grinding, Marinescu, I. B. (2004).

Snoeys, Maris and Peters (1978) observed from experimentation that the peak residual stress was directly related to the grinding zone temperature and so the maximum residual tensile stress can be controlled by application of the thermal models presented in the previous sections.

2.4.2 Workpiece Burn

This is the one of the most common type of thermal damage. It is generally associated with steels but can occur with other metallic materials as well, Malkin (1989).

Burn is characterised by oxidation colors (or temper colours) that form on the surface of the workpiece. These are indicators of microstrucural changes that can compromise the mechanical properties of the finished component. Dark blue colours are produced at high temperatures and are indicative of serious thermal damage, example of which can be seen in figure 2.11.

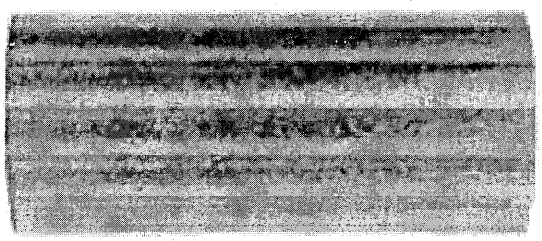

Figure 2.11: The Dark Blue Striping Effect Referred to as Burn, Marinescu, I. B. (2004).

This type of damage relates to the formation of un tempered martensite (UTM) in steels and can occur in steels in both hardened and unhardened state. The surface of the steel being ground is heated past a threshold value (that can be observed from the phase diagram in figure 2.12.) leading to the formation of martensite. The material is quenched due to the low temperature of the bulk material and the flow of coolant and so the material remains in this form. Martensite is extremely brittle and susceptible to cracking and so, it is likely to reduce any component to scrap. This UTM formation of an abusively ground sample can be clearly seen as white layer in figure 2.13. The hardness profile of a specimen damaged in this way can is presented in figure 2.14. Notice that deeper below the surface, where temperatures did not reach the critical threshold, softening or over tempering has occurred.

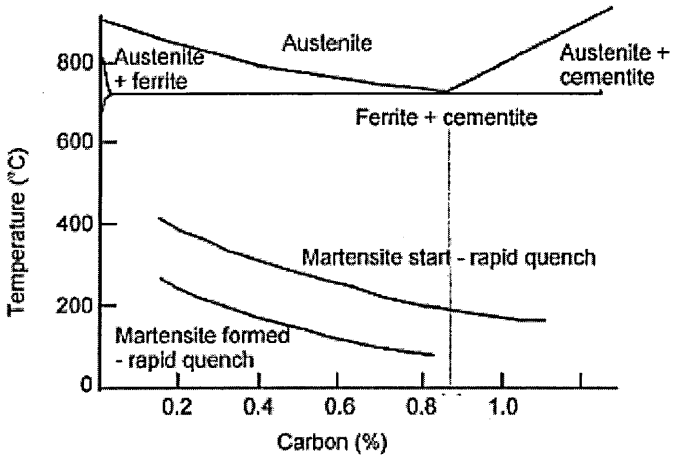

Figure 2.12: Iron – Carbon Phase Diagram, Marinescu, I. B. (2004).

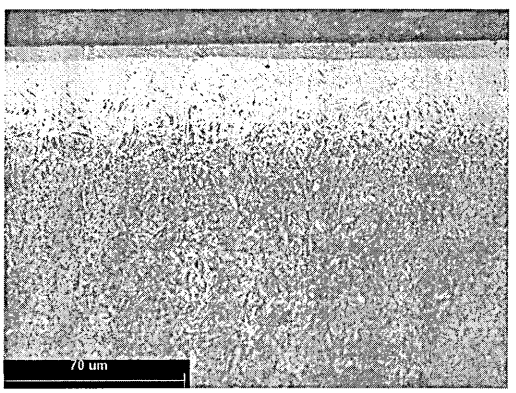

Figure 2.13: Formation of White Martensitic Layer, taken from work performed by Dr Jin of Cranfield University.

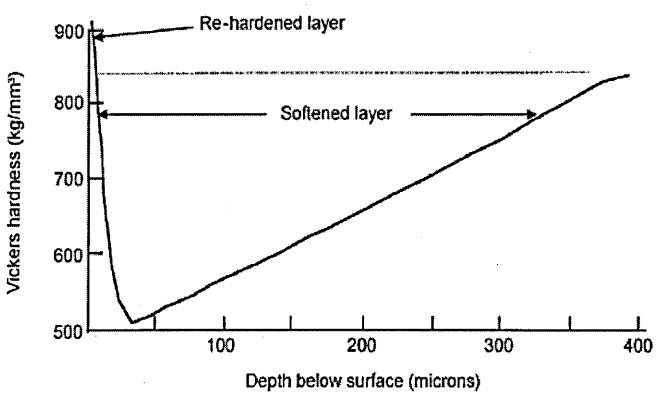

Figure 2.14: Hardness Variation in Steel due to Heavy Thermal Damage, Marinescu, I. B. (2004).

At lower temperatures a straw like colour is often witnessed, which is indicative of a lightly burned surface. This level of damage is likely to result in over tempering or softening of a previously hardened and tempered steel, Marinescu, I. B. (2004). An example of this can be seen from the etched and polished sample shown in figure 2.15, the dark layer is indicative of the formation of over tempered martensite (OTM). A plot of the reduction in hardness through the surface of a ground steel component can also be seen in figure 2.16.

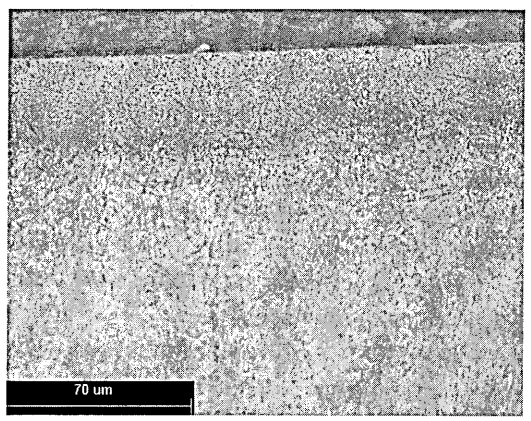

Figure 2.15: Over Tempered Steel, taken from work performed by Dr Jin of Cranfield University.

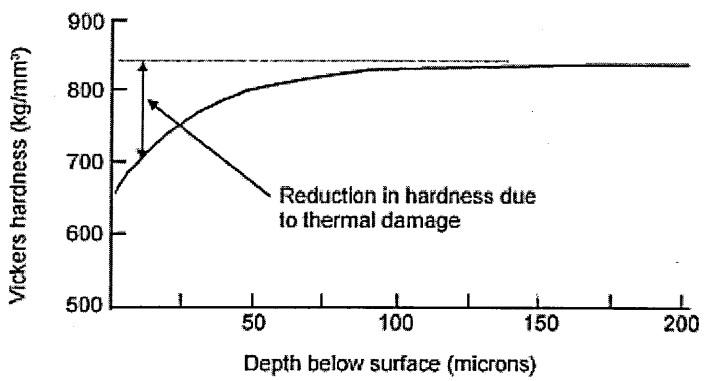

Figure 2.16: Hardness Variation in Steel due to Light Thermal Damage, Marinescu, I. B. (2004).

Thus the main types of thermal damage resulting from grinding have been summarised.

CHAPTER 3: PRELIMINARY SYSTEM DEVELOPMENT

The main focus of this work is to create a system that is capable of assisting production engineers in process design by selecting conditions that maximise the production rate whilst maintaining the integrity of the workpiece. Furthermore the system should also monitor grinding processes in real time to warn when process conditions approach thermal damage thresholds so that these may be avoided. This chapter details the development of this system and begins with a review of research work in predictive and reactionary measures to prevent the occurrence of thermal damage.

3.1 Evaluation of Existing Predictive Systems

The majority of work in this area involves some element of artificial intelligence to model the process and make relative rather than absolute recommendations for production engineers. This due to the complexity of the process that requires highly sophisticated analytical models if they are to make accurate predictions, Ali (2003).

An example of a rare analytical model used in parameter selection is that proposed by Midha (1991). It uses a model proposed by Malkin (1989) to test for the tendency for burn to occur. Malkin (1989) proposed that the burn threshold specific grinding energy is given by the expression:

$$f = \left(d_e^{1/4} a_c^{-3/4} v_w^{-1/2}\right) \qquad (3.1)$$

(Where d_e represents effective wheel diameter, a c depth of cut and v w the workpiece speed.)

When plotted as a graph the function yields a straight line where the gradient is related to the grinding temperature and a specific energy that falls above the line indicates that burn is likely to occur. This particular system then uses a model based on the predicted tangential cutting force to calculate the specific energy. An example burn threshold graph can be seen in figure 3.1.

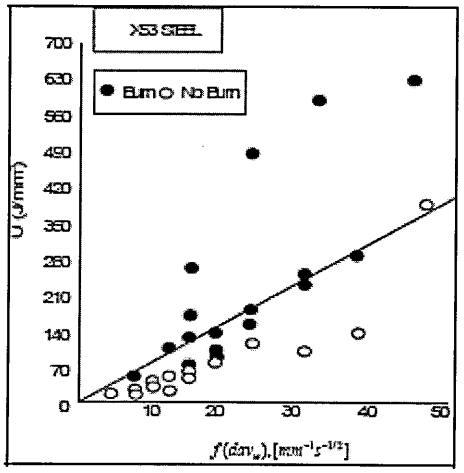

Figure 3.1: Shallow Cut Burn Threshold Specific Grinding Energy, Johnstone (2002).

This model is only applicable for shallow cut grinding and so is of little use in a modern machine shop that makes use of the productivity gains of HEDG or creep feed grinding. This approach is therefore not a viable solution.

Another approach is the use of expert or knowledge based systems. These contain a database of process knowledge from which the software draws inferences and makes recommendations to the user. Examples of this approach are given by Trmal (1992) and Koenig (1991).The process knowledge is normally stored in the form of Boolean rules, which are generated by using rule generation software to process experimental data or by the use of a human expert.

Ali (2003) used a fuzzy logic enhancement of this type of system for the prediction of grinding burn. The use of fuzzy logic provides an interpolation between the absolute rules by the use of fuzzification of the control parameters and membership functions. The inferences are then combined into a final result and provide an overall probability of burn occurrence.

The limitations of the Artificial Intelligence Systems are in the generation of the rule base. Ali (2003) points out that the use of a human expert produces rules that are subject to the preconceptions of the human; hence there are no guarantees that the human expert will be correct. The use of experimental data only provides accurate information about the exact conditions that have been tested. Fuzzy logic can be used

to extend inferences from these cases to new conditions. The use of shape functions provides an interpolation between the known points but this can only be within a reduced confidence level.

An error in the rule base generated by Ali (2003) illustrates these problems of artificial intelligence based systems. The rule base takes no account of HEDG conditions inferring that shallow cut depths and slow workpiece speeds are generally likely to reduce the occurrence of burn. The reason for this is that the test conditions used to generate the rule base did not extend to consider HEDG conditions where the occurrence of burn is reduced by imparting more energy to the grinding chip. Hence the use of this system will often result in sub optimal production rates.

3.2 Evaluation of Existing Reactionary Systems

Tang et al. (1980) used a graphite-infiltrated wheel for the prediction and control of workpiece burn. The graphite-penetrated wheel and the workpiece form a natural thermocouple, whereby the real temperature at the grinding zone, and subsequently the grinding burn, can be monitored. However, ordinary wheel materials are non-conductors and so the method is impractical in a real production environment.

Eda et al. (1992) used an acoustic emission (AE) signal for in-process identification of grinding burns. They found that AE around the frequency range of 10 kHz shows large power density when the abrasive grains are new, but decreases as the grains become worn and grinding burn proceeds. Aguiar (1997) established the DPO parameter for detection of burn in surface grinding. This parameter is the multiplication of the standard deviation of the RMS AE signal for each grinding wheel pass by the maximum value of the power level in the current pass and is said to increase until a threshold value is reached that indicates grinding burn. It therefore combines power monitoring with AE monitoring to provide a broader indication of the state of the process than AE alone. Despite this both methods rely on an empirically derived threshold. As was illustrated by the example given in section 3.1, this threshold is only certain within the experimental range and not universally applicable. The flexibility of an analytical tool is therefore lacking.

Another approach employs the characteristic analysis of the grinding temperature collected by an infrared measuring instrument; Huang Ren et al. (1992) presented a recognition technique to identify grinding burn in real time. Again this relies on an empirical threshold and so the same criticisms stand. In addition it has been noted that the presence of chips and coolant make this measurement difficult.

Malkin (1989) has also suggested a technique for the in-process control of burning that involves the monitoring of net grinding power, calculating the specific energy and comparing it with the threshold burning specific energy [2]. This threshold is derived from equation 3.1 and as stated is only applicable to shallow cut grinding.
Rowe (1988) proposed a similar system based on more sophisticated thermal models although it is still not applicable to HEDG as it does not use the circular arc of contact model described in chapter 3. The thermal models were used to calculate a threshold specific energy based on a single workpiece temperature threshold. Work by Jin and Stephenson (2005 b) demonstrate that the burn mechanism is more complex and so this approach is not valid. However, these power based techniques do have the advantage of requiring relatively cheap instrumentation as opposed to the infra red and AE approaches.

3.3 Current Work at Cranfield University

The School of Industrial and Manufacturing Science within Cranfield University have already developed a system for the prediction and monitoring of grinding temperatures based on the thermal models presented in section 2.4. The system has produced estimated grinding temperatures that correlate well with measured values, Walton (2005).

However it has a number of limitations:

- The temperature in both predictive and monitoring modes is not evaluated by the system to create an inference as to whether thermal damage will occur and so it is down to the knowledge and experience of the user to determine if the grinding conditions are optimal or not.

- The predictive system only enables the user to select one grinding condition and calculate a finished workpiece temperature; it does not allow the user to make comparisons with alternative conditions to assist in optimising the process. (Comparing variations in specific material removal rate would be particularly useful in HEDG conditions.)
- The monitoring system is not fast enough to evaluate grinding temperatures in real time and therefore cannot be used to prevent the onset of thermal damage. This also makes it slow to estimate multiple grinding temperatures for different conditions when used for prediction.
- The system relies on software written in LabView for the user interface and data acquisition with MatLab software performing all of the calculations; this has implications on system stability and speed. It also requires the user to have licences for both packages increasing the commercial cost of the system.

3.4 Conclusions from Study of Existing Systems

It seems that the majority of the work has relied on extracting inferences from empirically derived data, in the form of a rule base or by correlating an effect with some parameter that may be monitored. As illustrated by the rule base generated by Ali (2003) that did not address HEDG conditions, this can only be descriptive of the process in the range of conditions that the data was collected for. It is not always indicative of what happens outside this range or even between the data points. That is not to say that this method should be disregarded completely as it is likely to provide a good indication for the conditions it has been calibrated for.

An analytical approach should be more flexible. Consideration of the work that involved analytical models such as those of Malkin (1989) and Rowe (1988) are too simplistic in terms of the thermal model and the single specific energy threshold used. The system developed at Cranfield University, with its more sophisticated thermal models, is able to make accurate predictions of temperature but is of limited use for parameter selection and does not evaluate this in terms of the likely occurrence of burn, nor is it fast enough to do so.

This suggests that it would be prudent to design a system that uses both sophisticated analytical models for flexibility and empirically derived indicators when working under known conditions.

If such a sophisticated analytical approach is to be used its processing speed must be improved and strategies to evaluate the temperature in order to pre-empt the occurrence of thermal damage must be developed. It is also necessary to develop a system that allows the user to select optimal conditions by displaying multiple grinding conditions.

3.5 Burn Thresholds for Steel

For the purpose of this work we will restrict ourselves to the consideration of the most serious form of thermal damage, grinding burn.

The thermal models presented in section 2.3 can be used to estimate the finished workpiece temperature. A number of researchers have sought to find a threshold temperature, for the finished workpiece surface, beyond which the surface of the workpiece is burnt. McCormack et al (2001) for example found this to be 450°C for most steels where as Jin and Stephenson (2002) found a temperature of 400°C to coincide with burn for 51CrV4 high carbon steel. Rowe (1988) used this single temperature comparison technique to determine whether burn had occurred.

However as described in section 2.4, burn is a tempering process and so is dependant on the time of exposure as well as the temperature. Later work by Jin and Stephenson (2005 b), took this into account and introduced a tempering parameter:

$$P = T \cdot (k_1 + \log t) \qquad (3.2)$$

Where:

P: Tempering Parameter (Approximately 9300 for Carbon Steel)

T: Threshold Temperature

k_1: Constant (20 for Carbon Steel)

t: Exposure Time (Hours)

This equation enables the threshold temperature for a given time of exposure to be calculated.

The time of exposure of an arbitrary point on the workpiece surface is dependant on the workpiece speed and the contact length as follows, Jin and Stephenson (2005 b):

$$t = l_c / V_w \qquad (3.3)$$

Therefore a faster workpiece velocity allows a higher temperature to be generated without burn occurring, this effect should be taken into account in process planning.

Marinescu (2004), in the book "Tribology of Abrasive Machining Processes" suggested that the length over which the workpiece is exposed to heat, maybe three times that of the actual contact length and so it could be argued that equation 3.3 should include a multiplier of three.

Equations 3.2 and 3.3 provide a realistic condition from which the finished workpiece temperature can be evaluated. From the conclusion of section 3.4 the system should also include an empirically derived threshold so that the grinding process can be evaluated against known conditions, where possible, which we may be more accurate than the theoretical approach alone. As suggested in section 3.4 many of the empirical indicators used such as AE require expensive instrumentation and so should be disregarded. Since it is already necessary to monitor power to calculate the finished work piece temperature it is sensible to use an empirical indicator which is also derived from power.

Extensive grinding trials were performed at The School of Industrial and Manufacturing Science at Cranfield University across a range of grinding conditions for the high carbon steel 51CrV4. The trials covered conditions from shallow cut to HEDG with specific material removal rates from 2 to 200mm^3/mm.s. After each machining test the workpiece was inspected for burn and the net grinding power recorded. The total heat flux maybe simply calculated using equation 2.10. When this

was plotted against the specific material removal rate a distinct threshold was noted as can be seen in figure 3.2.

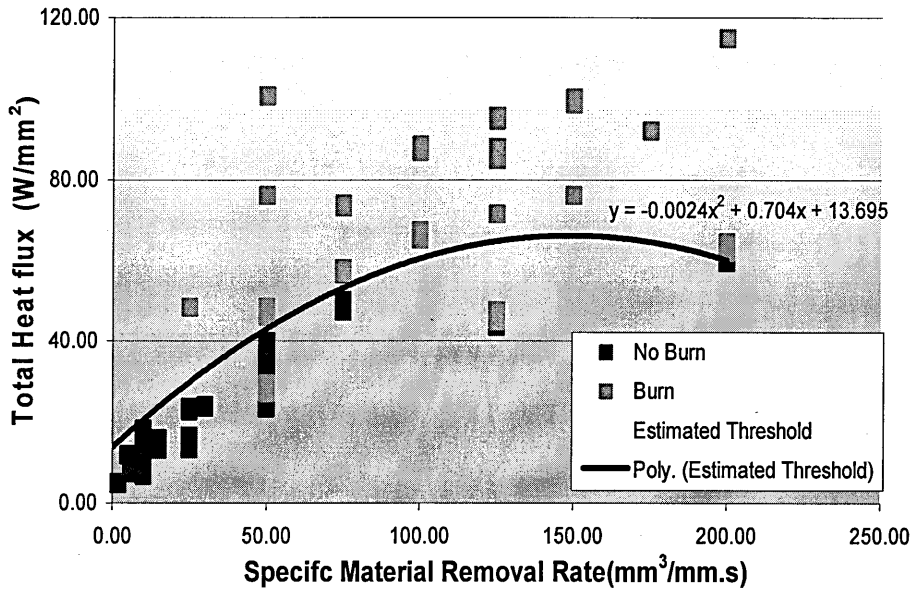

Figure 3.2: Experimentally Derived Burn Threshold Total Heat Flux.

The burn threshold was estimated with a quadratic curve which produces a good fit to the observed threshold (see equation 3.4). It is proposed that this curve can then be used as a heat flux threshold for burn in terms of the specific material removal rate.

$$\text{Burn Threshold } q_t = -0.0024 \,.\, Q'^2_w + 0.704 \,.\, Q'_w + 13.695 \qquad (3.4)$$

Clearly this should only be used in the range of specific material removal rates 2 to 200mm^3/mm.s that the threshold was developed for and the system that is to use this approach should warn when this condition is no longer valid. This prevents the errors noted in the 3.4 becoming an issue, as any user of the system would know to depend on the theoretical threshold when the valid range has been exceeded.

Both analytical and empirical indicators of grinding burn have now been described these can be used in the predictive system to select the optimum process parameters and to evaluate a grinding process in real time to prevent the onset of grinding burn. The theoretical burn temperature threshold that takes into account the tempering

parameter has not yet been used in a predictive system for parameter selection or an online monitoring or control system. The use of a combined theoretical and empirical threshold to increase the accuracy of burn prediction is also unique. The exact strategy in which these indicators will be used is developed in the subsequent sections.

3.6 The Approach to Software Design

National Instruments Lab View ™ is a graphical programming language that was originally intended specifically for test, measurement, and control. Since it now has the flexibility of a normal programming language with many higher level analysis and measurement tools it is ideally suited to this application that requires a data acquisitioned substantial mathematical and logical analysis. In this environment the system could easily be developed into an adaptive control system as classical and fuzzy logic control tools are available in Lab View.

Lab View has an inherent advantage for this application. Lab View sequences program execution by data flow; it performs each section of the program as soon as the inputs are available. Since the majority of the operations required to calculate the finished workpiece temperature are from static parameters it is simple to remove these from the real time flow of the program and have these calculations performed in advance. This is more difficult with a conventional text based language where sequencing does not allow parallel execution of functions.

A modular approach has been taken to software design as is recommended in one of the leading Lab View programming texts, Lab View for Everyone, Travis (2001). The complex overall system is built up from a hierarchy of smaller sub programs that perform specific functions. This assists the use of top down design, starting with the large functions such as the temperature calculation module that can then be broken down into convection factor calculating sub programs, final temperature estimation, specific material removal rate calculation and so on.

This also allows individual elements of the program to be developed and de bugged in isolation. These elements can then be reused multiple times in the program. This is

particularly useful as the parameter selection and monitoring systems share many common elements.

The modular approach makes the program easier to interpret and modify in the future. For example if an improved model for the estimation of a certain convection factor became available it would be simple to write a new sub program to calculate this parameter without disturbing the rest of the system.

The importance of the speed of program execution was also taken into account in the software design. Travis (2001) proposes rules for efficient Lab View programming: Local or global variables should not be used as these require memory allocation and a simple wired connection does not. Always define the size of an array when it is created as the system will create a memory allocation that defaults to the maximum allowable array size and so waste memory. This means that if a loop structure is used to generate an array by making an iterative calculation a "for loop" should be used opposed to a "while loop". This is because the number of cycles a "while loop" performs is indeterminate and so is the size of array it creates. These rules were rigidly adhered to through out this work.

Error monitoring was also built into the program from the outset, the program automatically checks that parameters have been selected and prompts the user when necessary. Warning messages are also given if the process conditions, input by the user, exceed the range in which the program is intended to function. The error messages explain the problem in plain English so it may be dealt with easily.

3.7 Overall System Architecture

Figure 3.2, overleaf, shows the overall concept of a single user interface with two separate systems; one to make predictions and assist the selection of grinding parameters and the other to monitor the grinding process, reporting on the state of the process and making recommendations. This part of the system could later be used as part of a constraint limited adaptive control system. The two functions will be described in detail in the chapters four and five.

The human machine interface (HMI) has many inputs common to both functions but most of the output indicators are specific to the mode of operation. These should be turned on and off with the operation mode to keep the user interface clear and uncomplicated. Each state of the HMI will be detailed in the section for the appropriate operation mode.

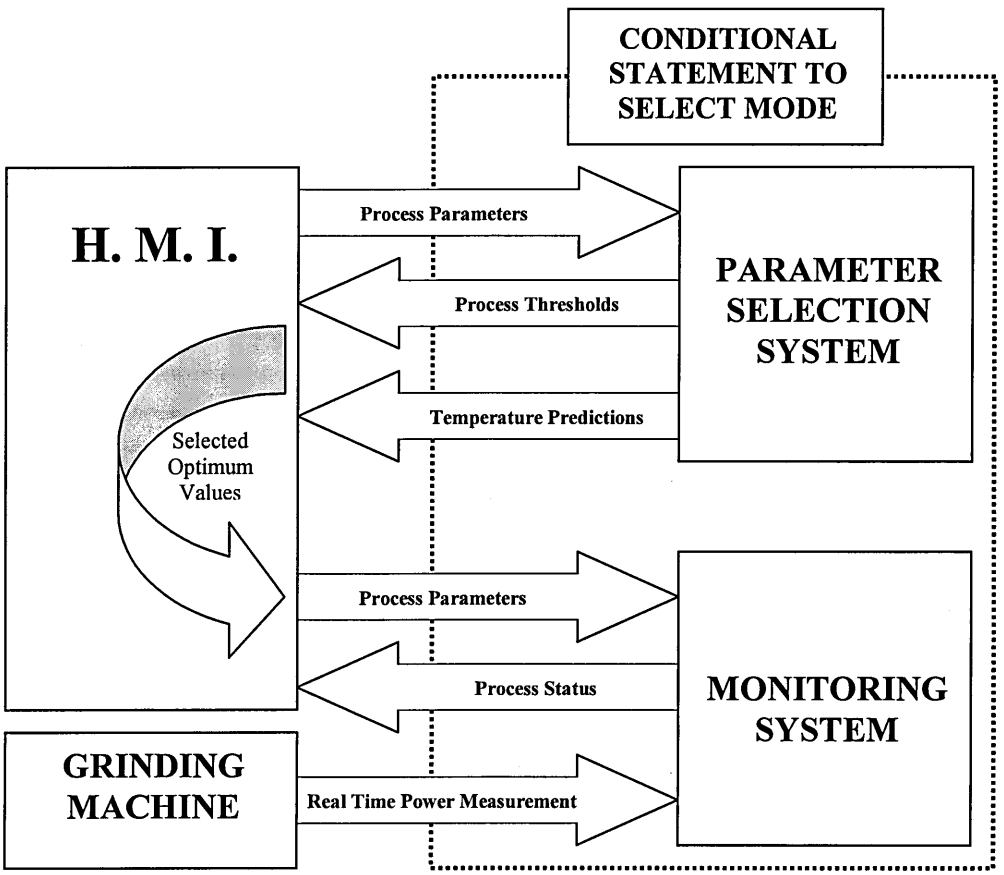

Figure 3.2: Overall System Diagram

CHAPTER 4: PARAMETER SELECTION SYSTEM DEVELOPMENT

As discussed in section 2.1.4 the specific material removal rate can have a profound affect on the finished workpiece temperature. Beyond a certain specific material removal rate increasing the depth of cut and workpiece speed imparts more heat energy to the chip. Increasing the cut depth has a corresponding effect on the distance from the point of maximum temperature to the finished surface and so can reduce the finished workpiece temperature. In section 3.5 it was also indicated that an increased workpiece speed may enable higher temperatures to be tolerated before burn occurs. It may be instinctive for a machine operator to reduce the workpiece speed or depth of cut if burn is realised. This can result in sub optimal production rates and could even increase the workpiece temperature and therefore worsen the resulting thermal damage.

The system should address this by calculating the finished workpiece temperature and the total heat flux for a range of material removal rates and display them graphically with the associated thresholds, detailed in section 3.5. The user should then be able to use a graphical selection tool to pick the optimum condition (i.e that with the highest removal rate below the threshold) and the system then presents the machine parameter that the condition relates to. This concept will become clearer with reference to the HMI and program structure in the following sections.

4.1 Parameter Selection System HMI

Figure 4.1 shows the HMI when used for parameter selection, this mode is selected using the switch in the top left. Around the outside of the screen are pull down menus that allow parameters such as the grinding geometry type or the wheel material to be chosen, the rest are numerical parameters that relate to the process conditions. There is also an increment input, a slider switch and Boolean control to select constant cut depth of workpiece speed. These set up the increment size and range over which the cut depth or workpiece speed are varied to create the variation in specific material removal rate for the calculations. The two graphs displaying the calculated temperatures, total heat flux and thresholds against specific material removal rate also can be seen. Notice the appearance of a single cursor that spans both graphs, this is

used to select the desired specific material removal rate and the resulting workpiece speed or material removal rate is displayed in the numeric indicators above the graphs. The position of the cursor is frozen by clicking the "make selection" button.

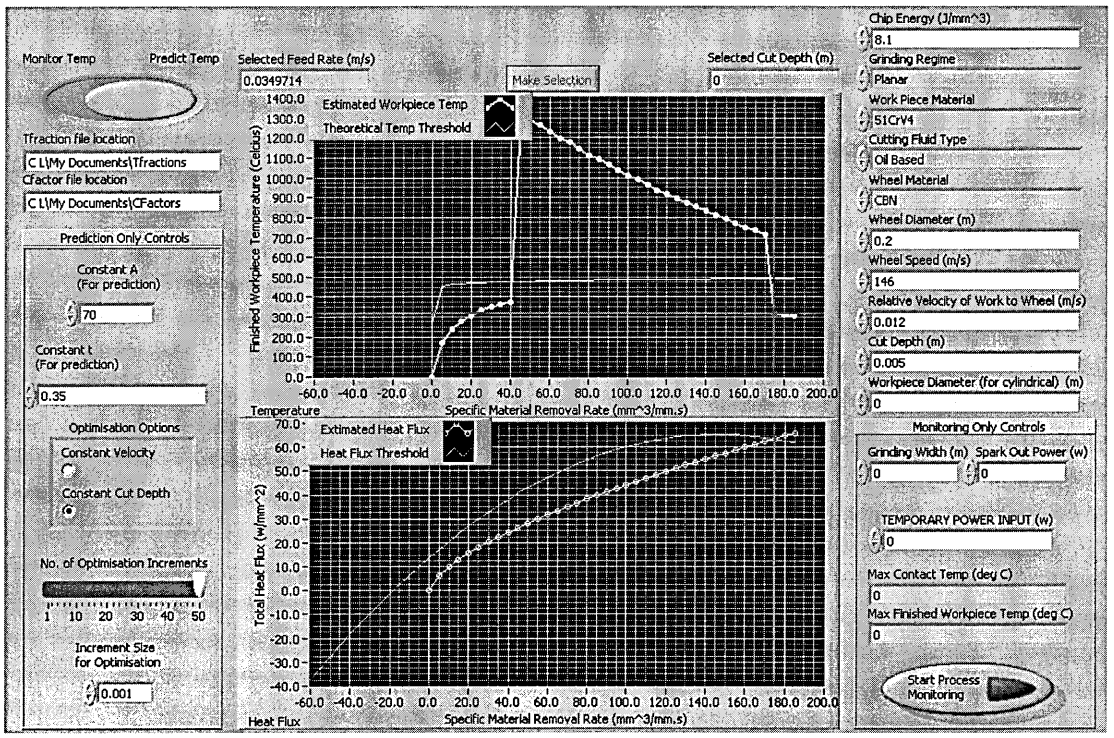

Figure 4.1: HMI for the Parameter Selection System

The graphs, numeric indicators and selection button are only displayed when in this mode; they are hidden when entering the monitoring mode of operation for clarity.

4.2 Structure of Parameter Selection System

A system diagram of the programs operation can be seen in figure 4.2 overleaf, note that the sequence of operation is indicated by the blue numbers. The logic of this structure will be explained in the text following this figure.

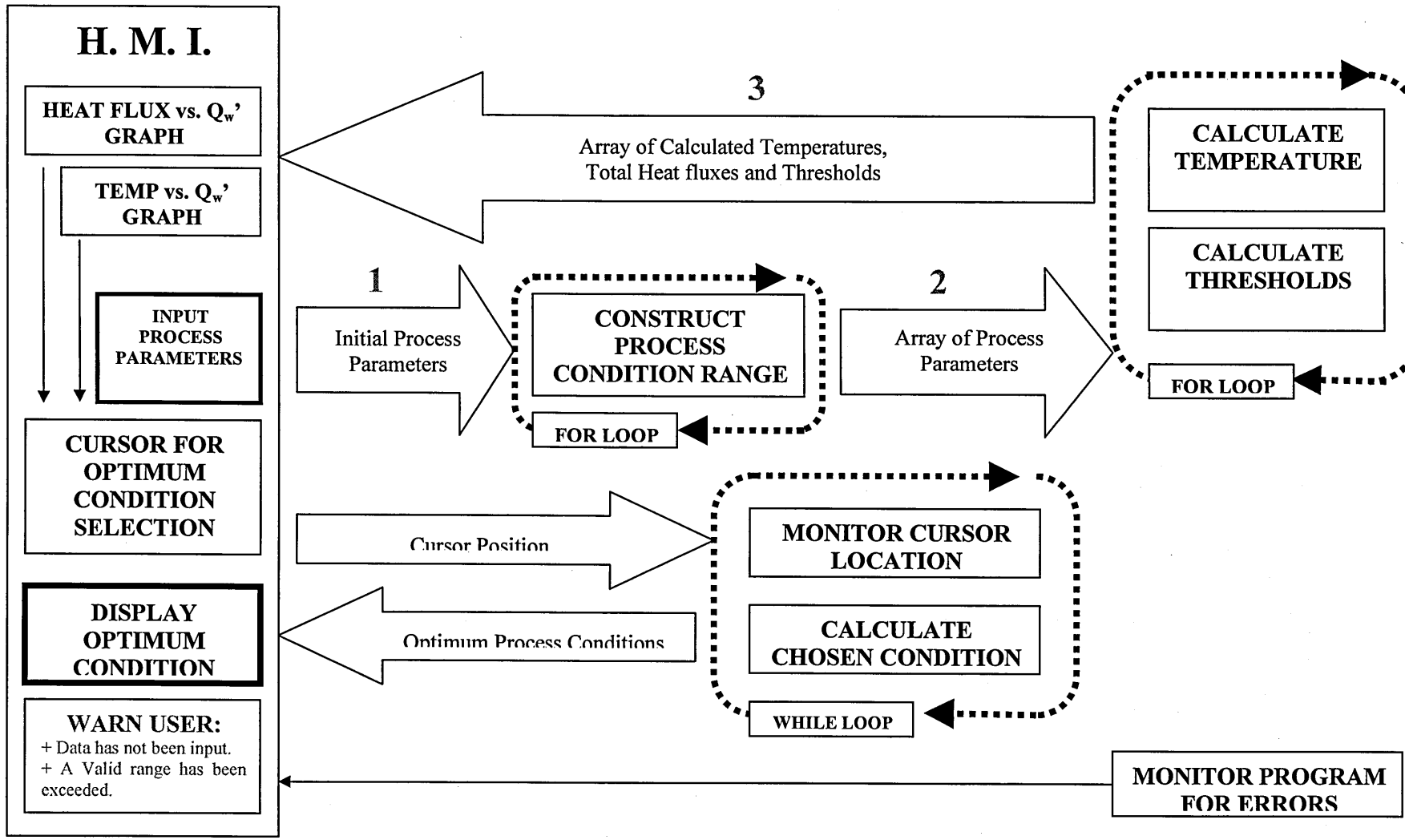

Figure 4.2: System Diagram of Parameter Selection System.

The user must start by selecting the predictive mode and then entering machine and process parameters. The first operation is to create the range over which calculations will be made. If constant cut depth is selected a "for loop" creates a range of workpiece speeds that are centred on the initial workpiece speed entered. Similarly, if constant workpiece speed is selected a range of cut depths are created. These are then output as a one dimensional array to the next "for loop" where the "calculate temperature" sub program produces a finished workpiece temperature and total heat flux for each condition. The associated thresholds are calculated in the same loop again for each condition, a system diagram of this operation can be seen in figure 4.3.

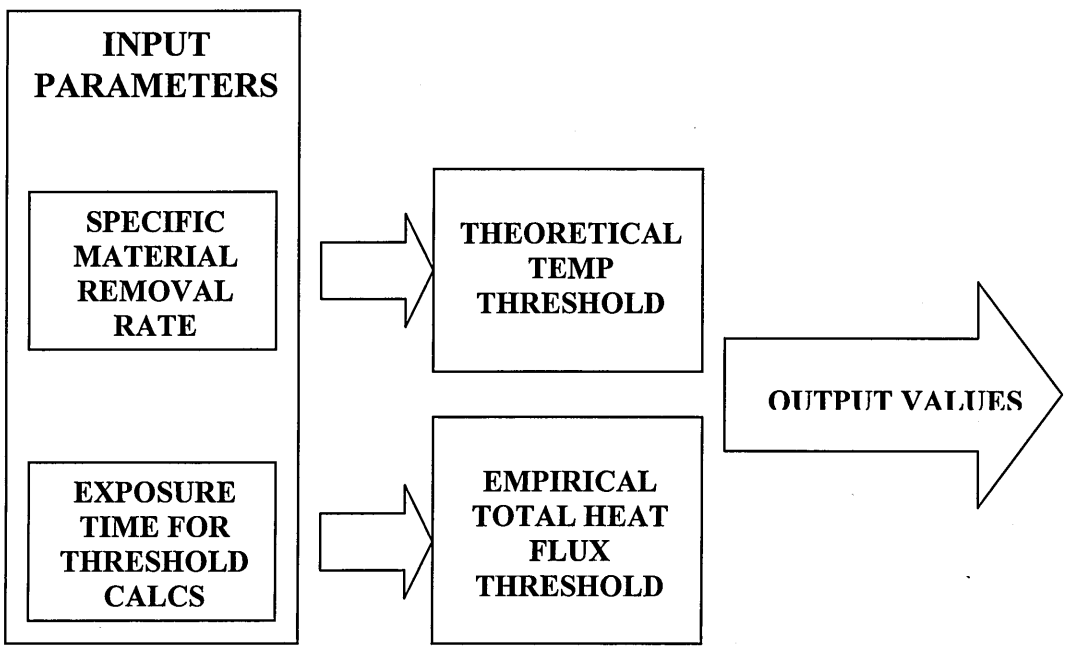

Figure 4.3: System Diagram of Calculation of Threshold Values for Both Parameter Selection and Monitoring Systems.

An array of finished workpiece temperatures, total heat fluxes and thresholds can then be output to the graphs on the HMI, so that the user may select the optimum condition.

There is a separate "while loop", in the bottom right of figure 4.2, responsible for controlling the selection cursor. There are actually two cursors (one for each graph) that the program creates a link between to give the appearance of only one. This enables the user to consider the empirical heat flux and theoretical temperature thresholds simultaneously. The loop monitors the cursor position along the x axis

where the specific material removal rate is plotted. From this it calculates the resulting workpiece speed or cut depth. The operation of this loop is continuous until the "make selection" button is pressed. This cancels the "while loop" and so the workpiece speed or cut depth is frozen on the HMI.

4.3 Calculate Temperature Sub Program

The "Calculate Temperature" sub program is large and complex containing two further levels of sub programs within it. It therefore requires further explanation. A system diagram of the Calculate Temperature sub program can be seen in figure 4.4 overleaf.

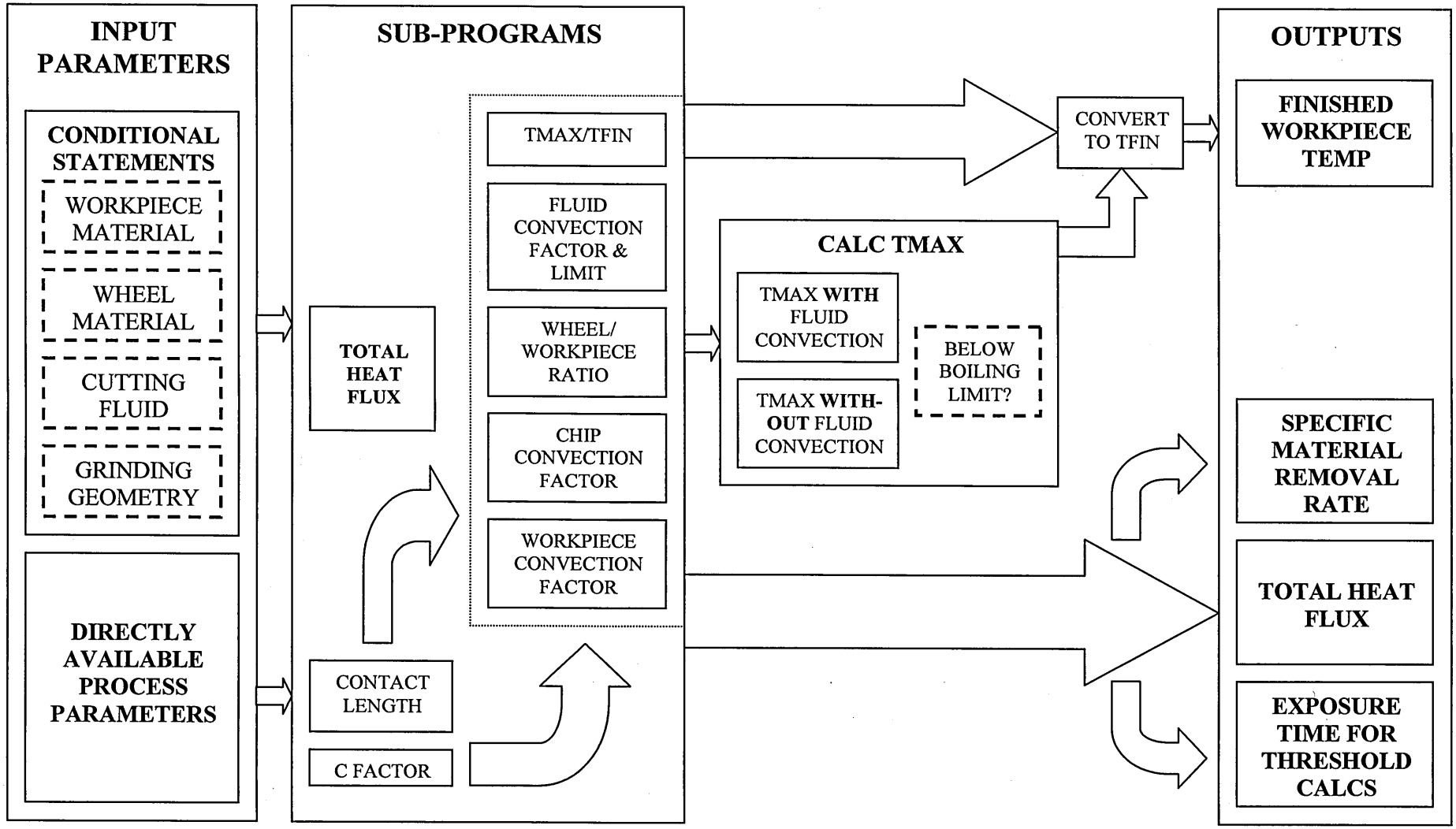

Figure 4.4: System Diagram of Temperature Calculation for Parameter Selection System.

The program begins by using conditional statements to output multiple numeric parameters to the rest of the program. These are controlled by the pull down menus on the HMI. For example, if the user selects the work piece material type to be 51CrV4 from the pull down menu the conditional statements outputs the thermal parameters for this material. In this way additional workpiece materials can easily be added to the software. If process parameters are directly available such as the wheel speed this number is passed immediately to next stage of the program for the calculations to be performed.

The next section of the program uses a number of sub programs and some additional basic math functions to calculate such things as the total heat flux and the convection factors. Most of these simply use equations detailed in section 2.3 and some are more complex warranting a more detailed discussion (i.e. C factor and chip convection factor calculation,) which are dealt with in the subsequent sections. The remaining quantities from figure 4.4 that have to be calculated are shown in table 4.1 with a list of the equations used.

Parameter	Equation	Comments
Specific Material Removal Rate, Q'_w.	2.12	Used in the calculation of specific energy and also to plot the temperature and total heat flux against for parameter selection.
Specific Grinding Energy, e_c.	2.11	Used in the calculation of the total heat flux.
Total Heat Flux, q_t.	2.13	Used in the calculation of grinding temperatures and also for the user to compare against the empirical heat flux threshold.
Contact Length l_c.	2.1-2.3	This subprogram is controlled by a conditional statement based on the process geometry; it uses a different equation for planar, external and internal cylindrical grinding. Used in the calculation of many convection factors and the calculation of the exposure time for the temperature threshold.
Workpiece wheel partition ratio, R_{ws}.	2.16	Used in the calculation of the maximum contact temperature in the next stage of operation.
Workpiece convection factor, h_w.	2.25	Used in the calculation of the maximum contact temperature in the next stage of operation. Requires the C factor to be calculated which is discussed in section 4.3.1
Fluid Convection Factor, h_f.	N/A	For speed of calculation the static values were chosen as opposed to the analytical approach. (See section 2.3.5) This method has been shown to provide a good estimation of grinding temperatures by Rowe and Jin (2001) b and many others. This method has the advantage of reducing the calculation time.

Table 4.1: Details of the Parameters Calculated in the Second Stage of Operation of the Sub Program "Calculate Temperature".

4.3.1 C Factor Estimation

From Section 2.3 it can be seen that the C factor is calculated from equations 2.4 and 2.3. Hence the estimation of the C factor requires the use of a modified Bessel function of the second order zero this function is very demanding on processor power. The fraction of contact to finished workpiece temperature (T_{con}/T_{fin}) must also be calculated in this way which increases this demand for processing power. This has been indicated as the main reason for the slow processing speed of the existing thermal monitoring system created by Cranfield University, Jin and Walton (2005 c). Therefore the calculation time for the C factor and T_{con}/T_{fin} must be reduced, if the overall efficiency of the system is to be improved in the calculation of multiple temperatures for parameter selection. This is even more important in the systems application to real time monitoring dealt with in Chapter 5.

The approach taken was to remove this calculation time from the run cycle of the overall program by using "look up tables". In this method a wide range of values are calculated in advance and stored in files, leaving the software to simply select the relevant value in the real time operation of the program. A system diagram of the sub program responsible for this operation can be seen in figure 4.5.

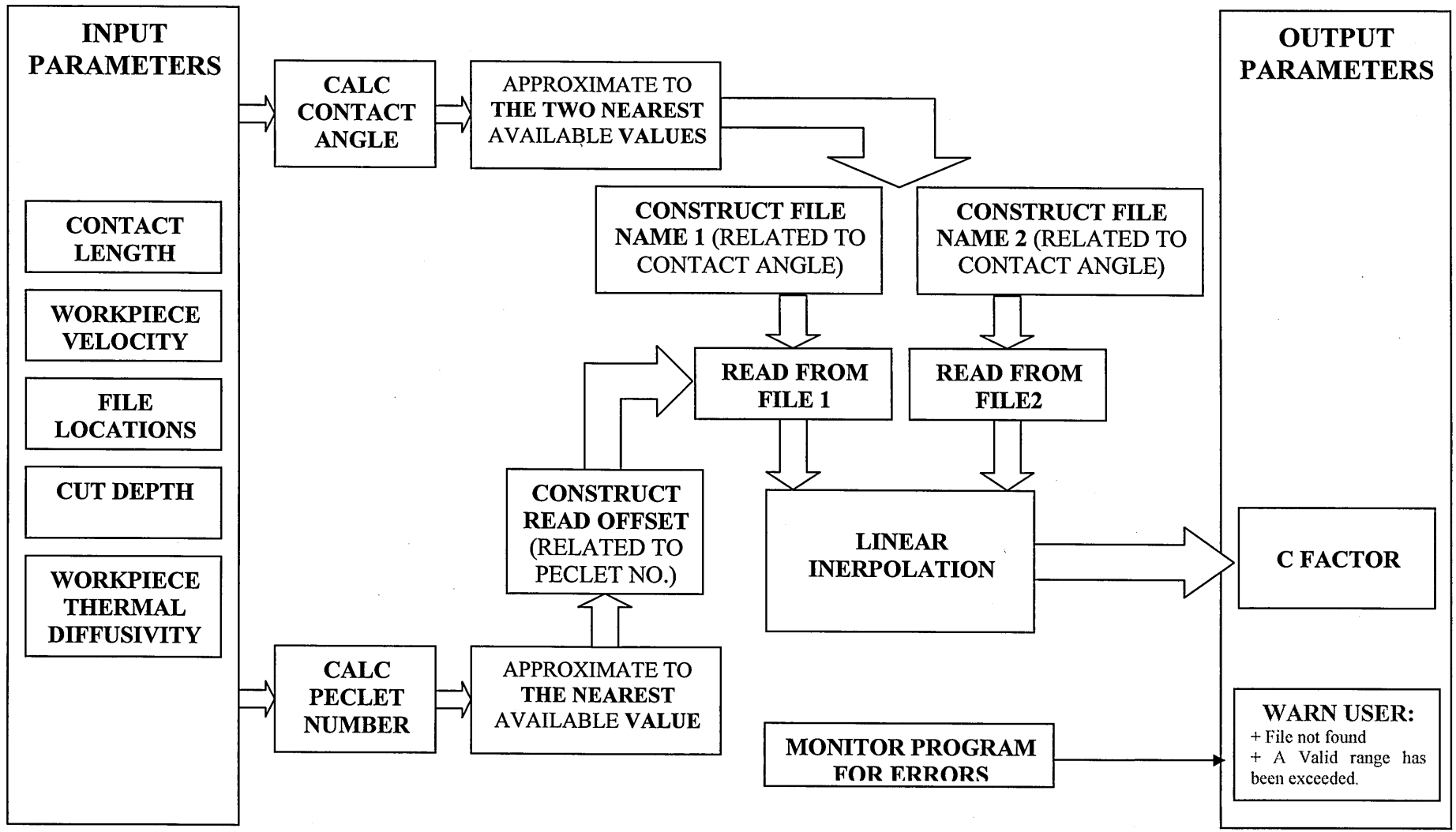

Figure 4.5: System Diagram of T_{con}/T_{fin} or C Factor Calculation Sub Program.

The C factor and T_{con}/T_{fin} are dependant on the Peclet number defined by equation 2.8 and the contact angle defined by ($\sin\Phi = a / l_c$). In implementing the "look up table" strategy it is necessary to determine a suitable range and resolution of these parameter values to cover the full range of likely grinding conditions within an acceptable accuracy. A range of 0.05 to 200 for Peclet number and 0.1° to 20° for contact angle was deemed to cover grinding conditions from shallow cut to HEDG. These values were then organised into one table of Peclet numbers per contact angle which were saved as text files. It is possible to enhance this accuracy without increasing resolution by using interpolation. The accuracy of the interpolation increases with the order of the function used at the expense of processing speed. Since processing speed is such an important consideration, accuracy was achieved through the use of a high resolution and a one dimensional linear interpolation. The use of a high resolution has no speed penalty and linear interpolation only requires a simple calculation to be made. Using only one dimension of interpolation requires that a higher resolution be utilised for the other dimension to compensate.

The next most important function of the program is to approximate the calculated values for Peclet number and contact angle to the nearest values available in the tables. This is performed by comparing the calculated values against a number of nested conditional statements and outputting the closest (or two closest values for the linear interpolation).

The same program can be used for both T_{con}/T_{fin} and C factor estimation with a minor modification to look for the "look up table" files in a different location. It is the values within the files that makes the program specific to a particular application.

The resulting sub program was validated against the analytical method by calculating a range of C factors and T_{con}/T_{fin} for contact angles and Peclet numbers that cover the full range of grinding conditions. The effect of contact angle and Peclet number was considered in isolation and small increments were tested in the middle of the range to check for discontinuities. Care was taken to ensure that input values did not coincide exactly with the look up table values and so the effect of the approximation and interpolation could be observed. Comparative graphs can be seen in figures 4.6 to 4.9

Figures 4.8 and 4.9 show a large deviation at low contact angles, this problem was solved by an increase the resolution, The effect of this improvement can be seen in figures 4.10 and 4.11. The tests subsequent tests demonstrated that the mean and maximum error, between the analytical and "look up table" methods, was now 0.13% and 1.89% respectively. This was deemed to be well within the expected accuracy of the overall system and so adequate for this application. The execution time for the program can also be recorded with Lab View, albeit with a limited accuracy, and this was found to be in the order of milliseconds for the look up table method where as the analytical calculation can take several minutes, Jin and Walton (2005).

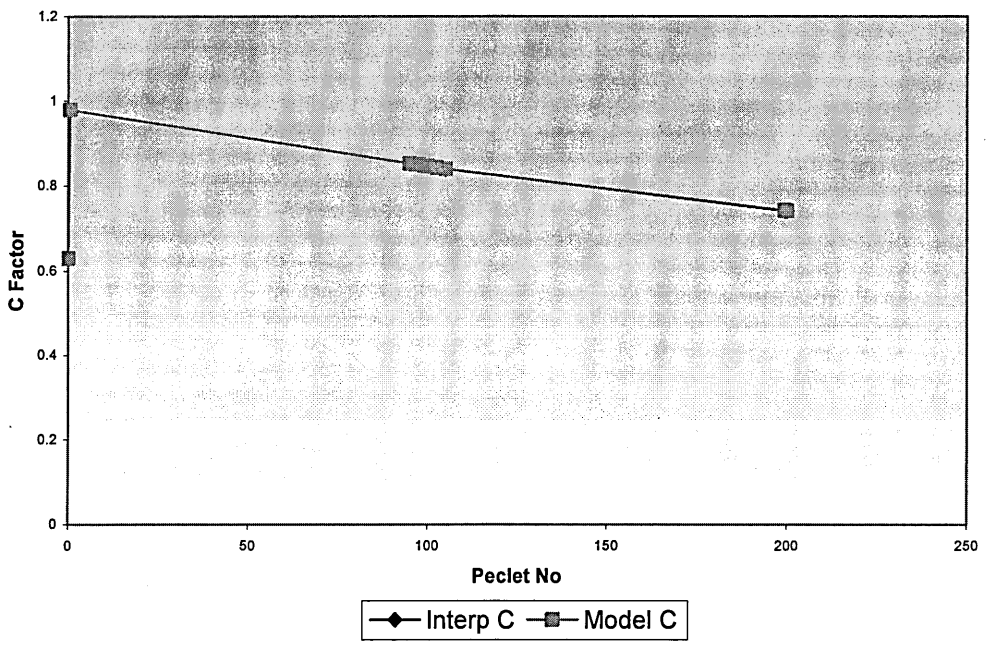

Figure 4.6: Comparison of C Factor Estimation Methods for Constant Contact Angle.

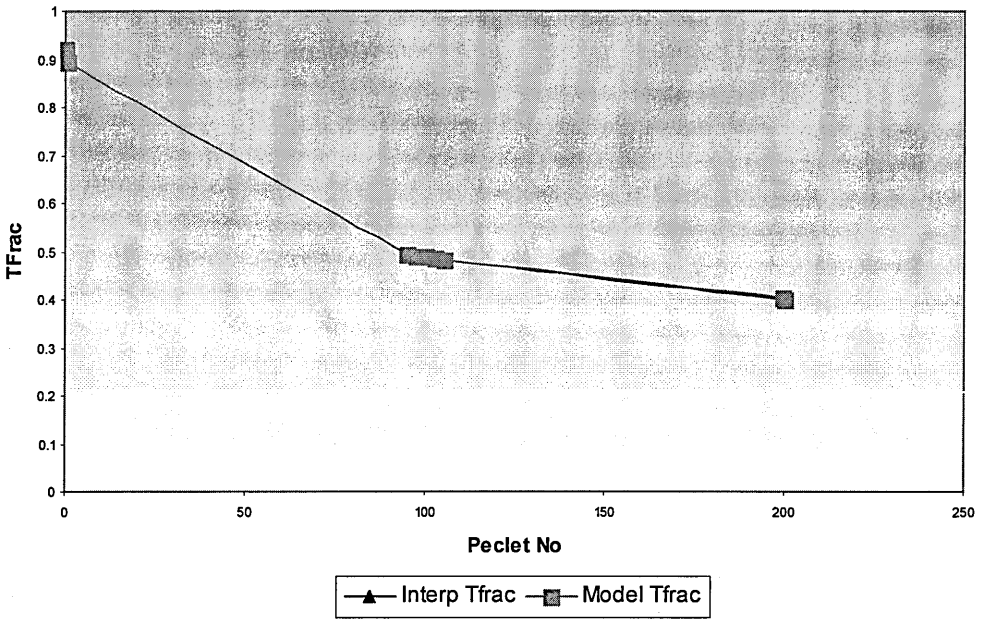

Figure 4.7: Comparison of T_{con}/T_{fin} Estimation Methods with Constant Contact Angle.

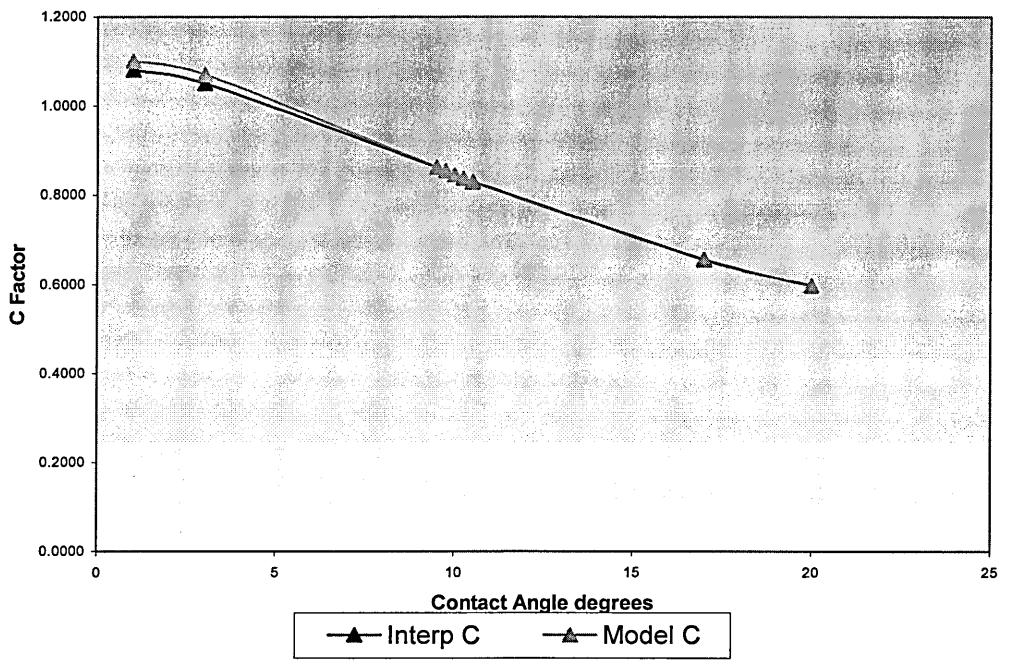

Figure 4.8: Comparison of C Factor Estimation Methods for Constant Peclet Number.

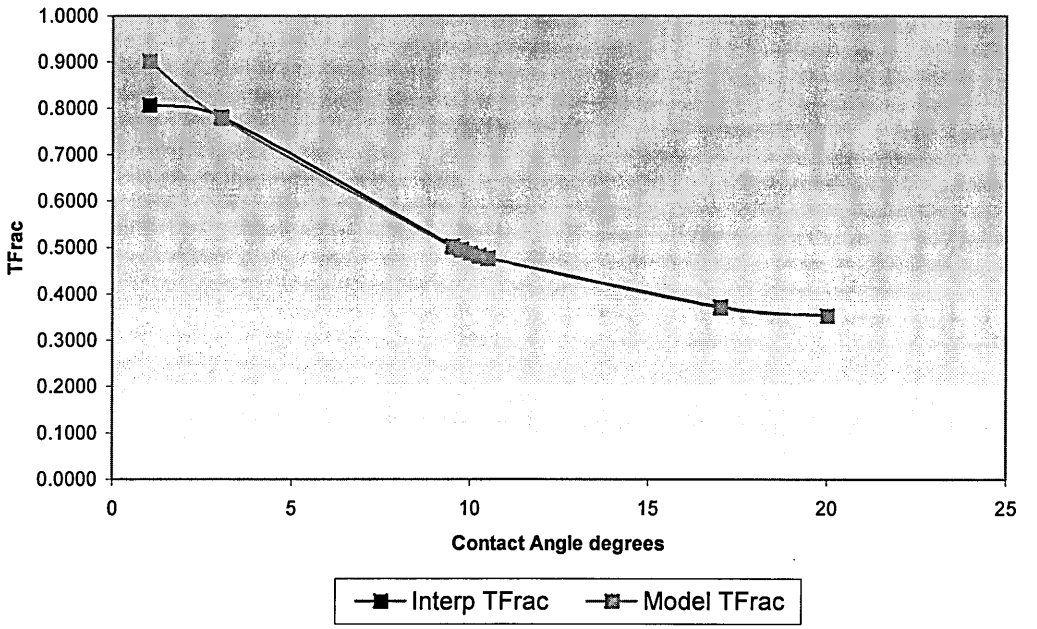

Figure 4.9: Comparison of T_{con}/T_{fin} Estimation Methods for Constant Peclet Number.

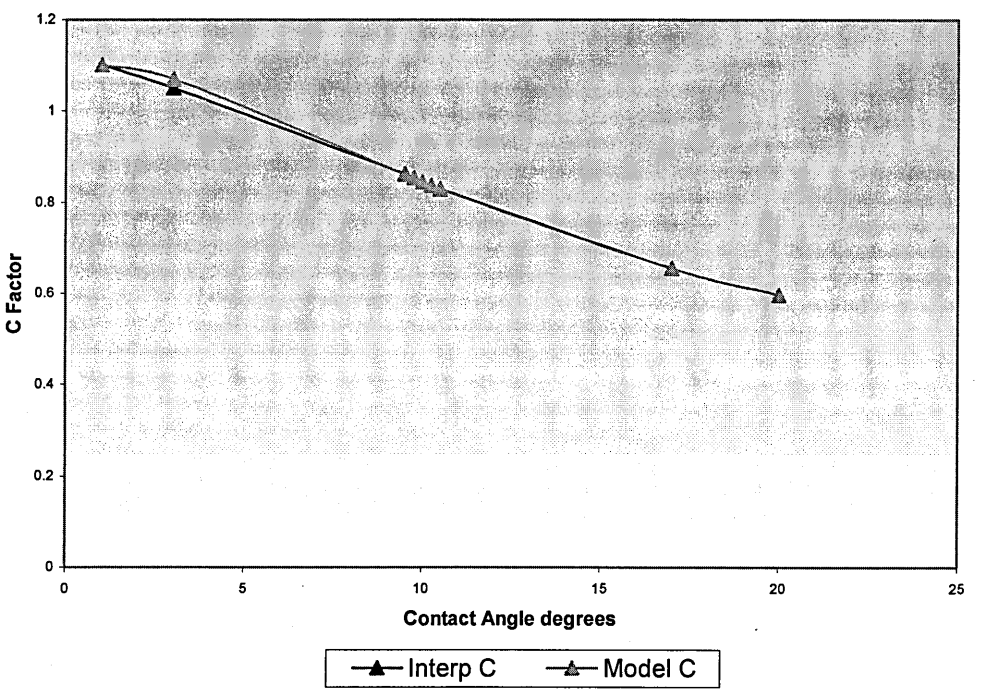

Figure 4.10: Comparison of C Factor Estimation Methods for Constant Peclet Number with Increased Contact Angle Resolution.

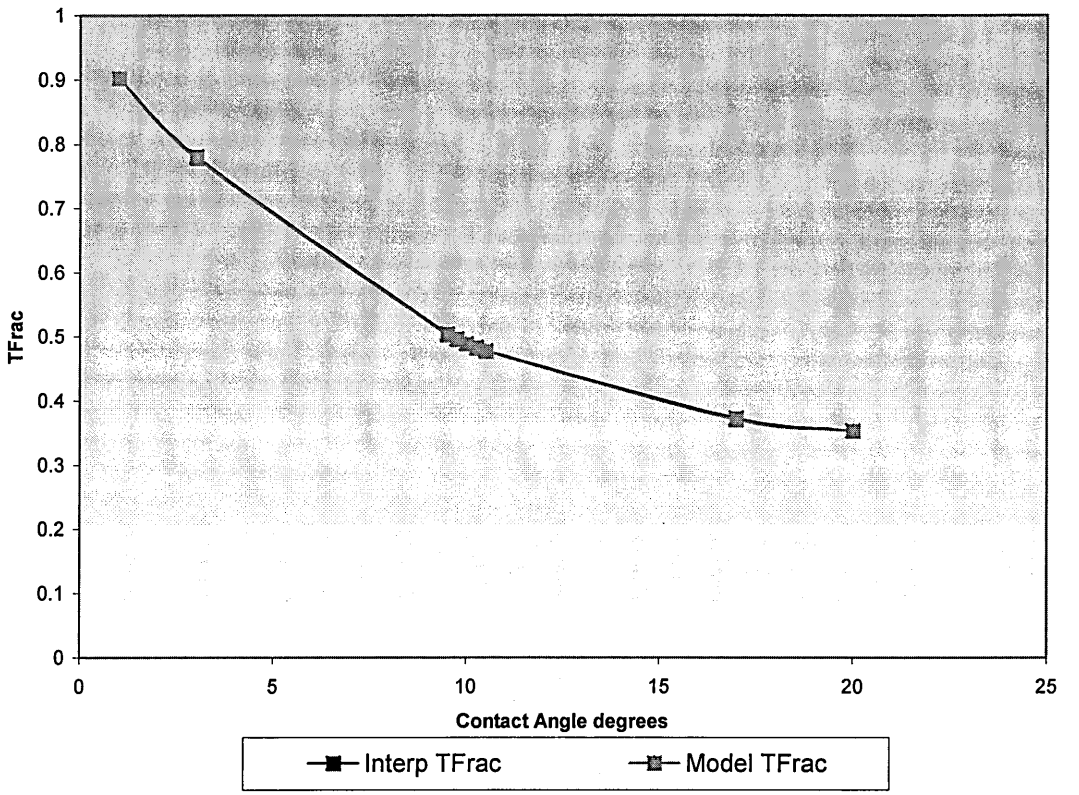

Figure 4.11: Comparison of T_{con}/T_{fin} Estimation Methods for Constant Peclet Number with Increased Contact Angle Resolution.

4.3.2 Estimation of Convection Factor to Chips

Section 2.3.6 describes three possible methods to estimate this convection factor.
The linear variation in chip temperature with maximum contact temperature model has been proven to provide a good approximation of the energy partitioned to the chips, Jin and Stephenson (2002) and (2005). However, its dependence on the maximum contact temperature requires an iterative calculation with a convergence test to be incorporated into any program that uses this model. Since speed is such an important requirement in this application, the method should be disregarded as it could increase the overall calculation time dramatically.

The use of equation 2.19 to estimate the energy partitioned to the chips based on a constant chip temperature close to the chip melting point does not take account of the variation in chip temperature across different grinding conditions that has been

demonstrated by Jin and Stephenson (2002) and (2005). However, it has been shown to provide good correlation with measured temperatures under certain conditions, Rowe and Jin (2001 b).

The formation analysis method is complex and not yet widely proven as it is so new. Therefore it would be unwise to base the system on this model at this stage. This complexity may also have a detrimental effect on speed and since the model has such a large number of parameters it does not lend itself well to a "look up table" approach as applied to the C factor calculation.

Therefore a method that provides simplicity and flexibility to adapt to the change in chip temperature across different grinding conditions is required. It is proposed that the use of equation 2.17 allows the user to specify the specific chip energy instead of inferring this with material properties and a chip temperature. The specific chip energy can then easily be changed without the need for the temperature dependence of specific heat capacity to be taken into consideration. This method gives the user greater autonomy to decide on the appropriate model to use for the grinding conditions. The user can then choose a specific chip energy based on experience or it can be taken from chip formation analysis model or the constant chip temperature model. The graph below shows a range of calculated values for the specific chip energy using the chip formation analysis model for some arbitrary grinding conditions. This could be used to assist in the selection of the correct specific chip energy.

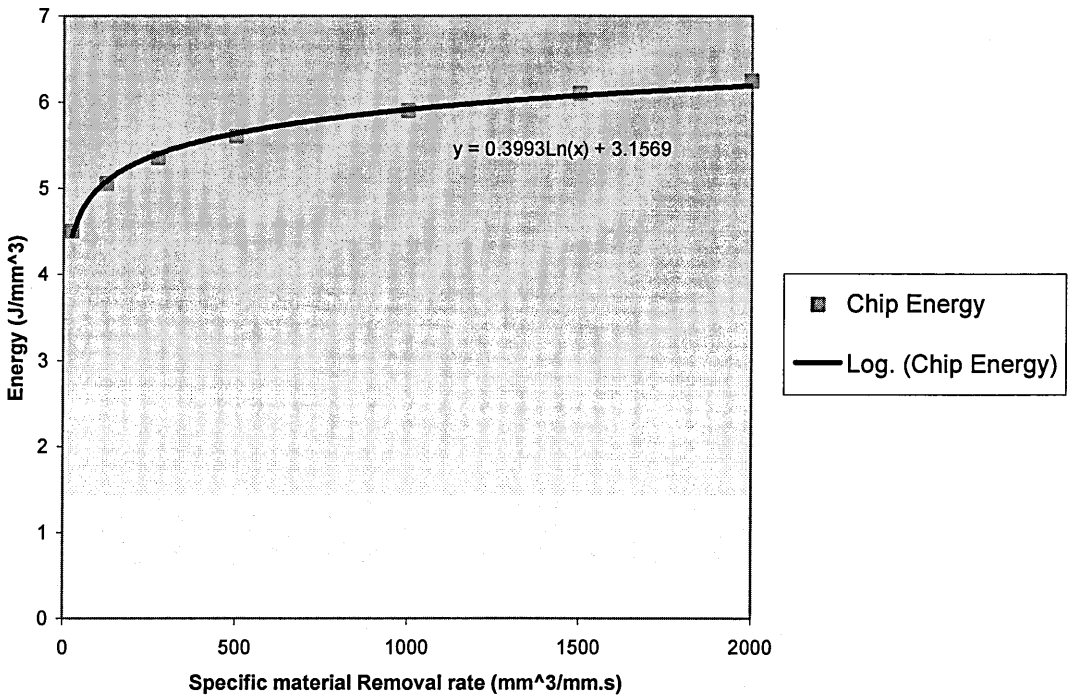

Figure 4.12: Variation in Specific Chip Energy with Specific Material Removal Rate Using the Chip Formation Analysis Model.

The modular approach to software design that has been taken should also allow the full chip formation analysis model to be simply incorporated into the system at a later date.

4.3.3 Estimation of Finished Workpiece Temperature

The sub programs calculation of all of the parameters necessary to estimate the maximum contact and finished workpiece temperatures have now been described. As can be seen in figure 4.4, another sub program is used to calculate the temperatures. The sub program is essentially based on equation 2.26, although the heat flux q_{ch} is used directly instead of using a separate chip convection factor and chip temperature. This results from the decisions made in section 4.3.2 on the method of estimation for the chip convection factor.

Reference to equation 2.26 and figure 4.4 show that the calculation of the maximum contact temperature is dependant on whether the burn out temperature has been

exceeded or not. When this has been exceeded the convection factor to the grinding fluid is assumed to be zero. This is simply integrated into the program functionality using a conditional statement. An initial calculation is made including the convection factor to the fluid, the temperature is then compared against the relevant burn out threshold. If it has been exceeded the conditional statement recalculates the temperature without ignoring convection to the fluid. If it has not the conditional statement passes the original value on.

The final action of the program is to multiply the maximum contact temperature by the fraction T_{con}/T_{fin} to obtain the finished workpiece temperature for the process parameter selection by the user.

CHAPTER 5: MONITORING SYSTEM DEVELOPMENT

The purpose of the monitoring system is to calculate the finished workpiece temperature and total heat flux and compare these with the thresholds derived in section 3.5. The system then provides the user with information about the state of the process and makes recommendations of any necessary course of action.

The monitoring system shares many common elements with the parameter selection system, such as the generic inputs on the HMI and many of the subprograms performing calculations within the program. The design of this system will be described beginning with the HMI.

5.1 Monitoring System HMI

The HMI designed for this purpose is displayed in figure 5.1.

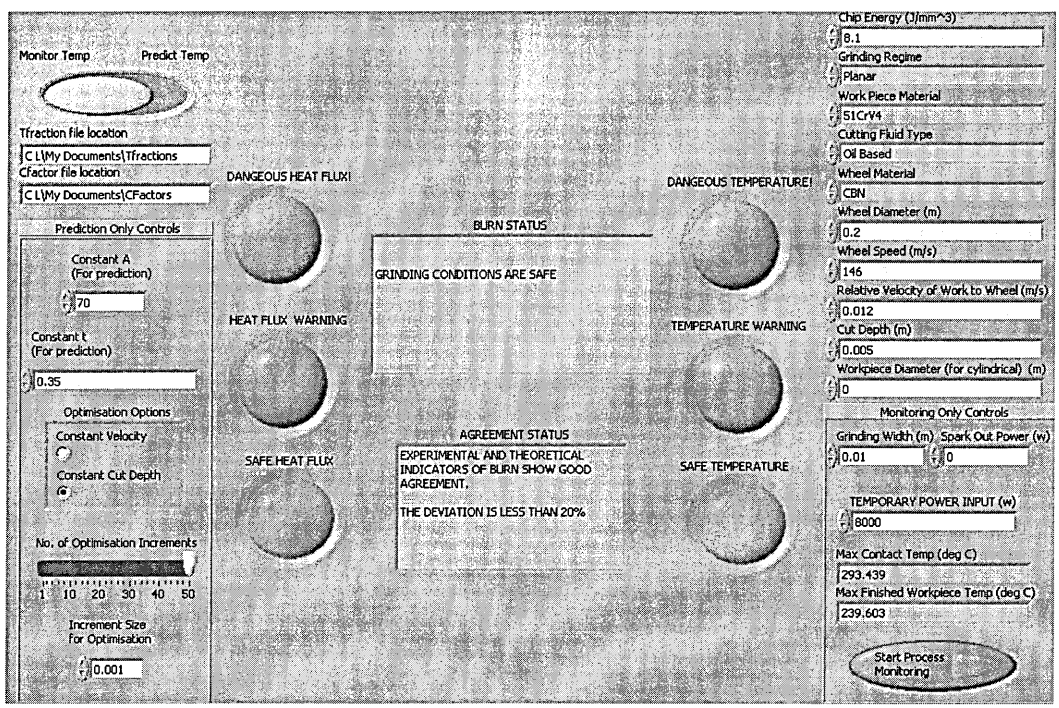

Figure 5.1: HMI for Monitoring System.

The philosophy behind the HMI is one of simplicity to present the user with concise easily interpreted information. A traffic light system was deemed to provide this:

Green indicates safe conditions, amber a warning that a threshold is being approached and red when a threshold has been broken. This dangerous condition is also accompanied by an audible alarm.

The central window provides more information to the user, explaining what the status means and making recommendations; revise parameters for optimisation, proceed with caution or stop immediately.

The agreement of the thresholds is also displayed and a warning flagged if the deviation is greater than 20%.

Again the valid range of the heat flux threshold should also be considered and a warning dialogue box is flagged before the program will run should the process be operating outside this range.

5.2 Structure of the Monitoring System

A diagram of the operation of the monitoring system is presented in figure 5.2

5.2.1 Pre Calculate Sub Program

From figure 5.2 it can be seen that the "pre calculate" sub program is outside of the real time loop. The convection factors, specific material removal rate, T_{fin}/T_{con} and the exposure time for the temperature threshold can all be calculated ahead of time to make the real time calculation more efficient. As stated in section 3.6, Lab View lends itself well to this type of structure because it is dataflow driven. A system diagram of this sub program can be seen in figure 5.3. It is clear from this diagram that its operation is largely the same as the "calculate temperature" sub program detailed in section 4.3 for the parameter selection system and so requires no further explanation. The main exception being that the "Calc Tmax" sub program is absent as this must be continually re-evaluated in real time.

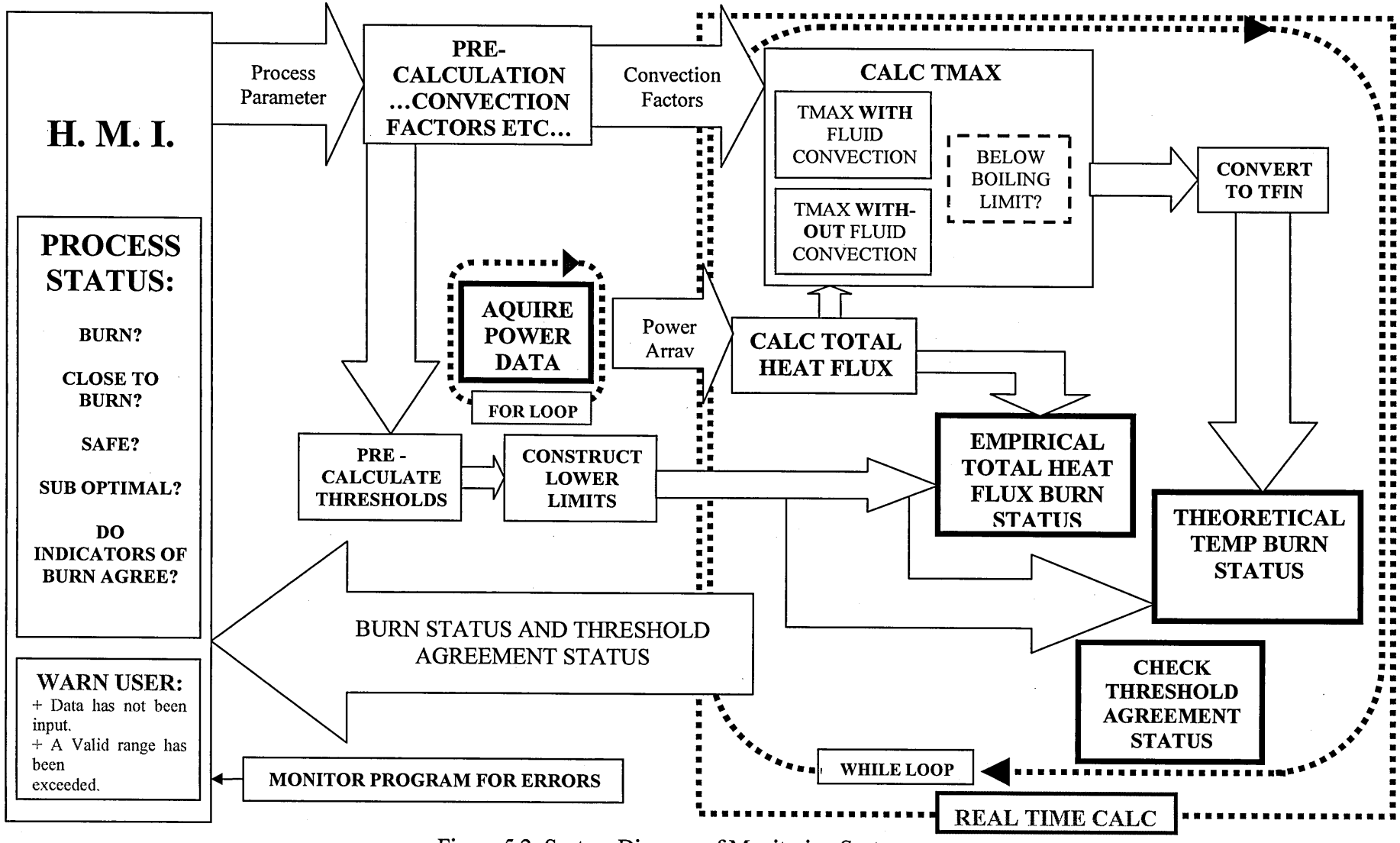

Figure 5.2: System Diagram of Monitoring System.

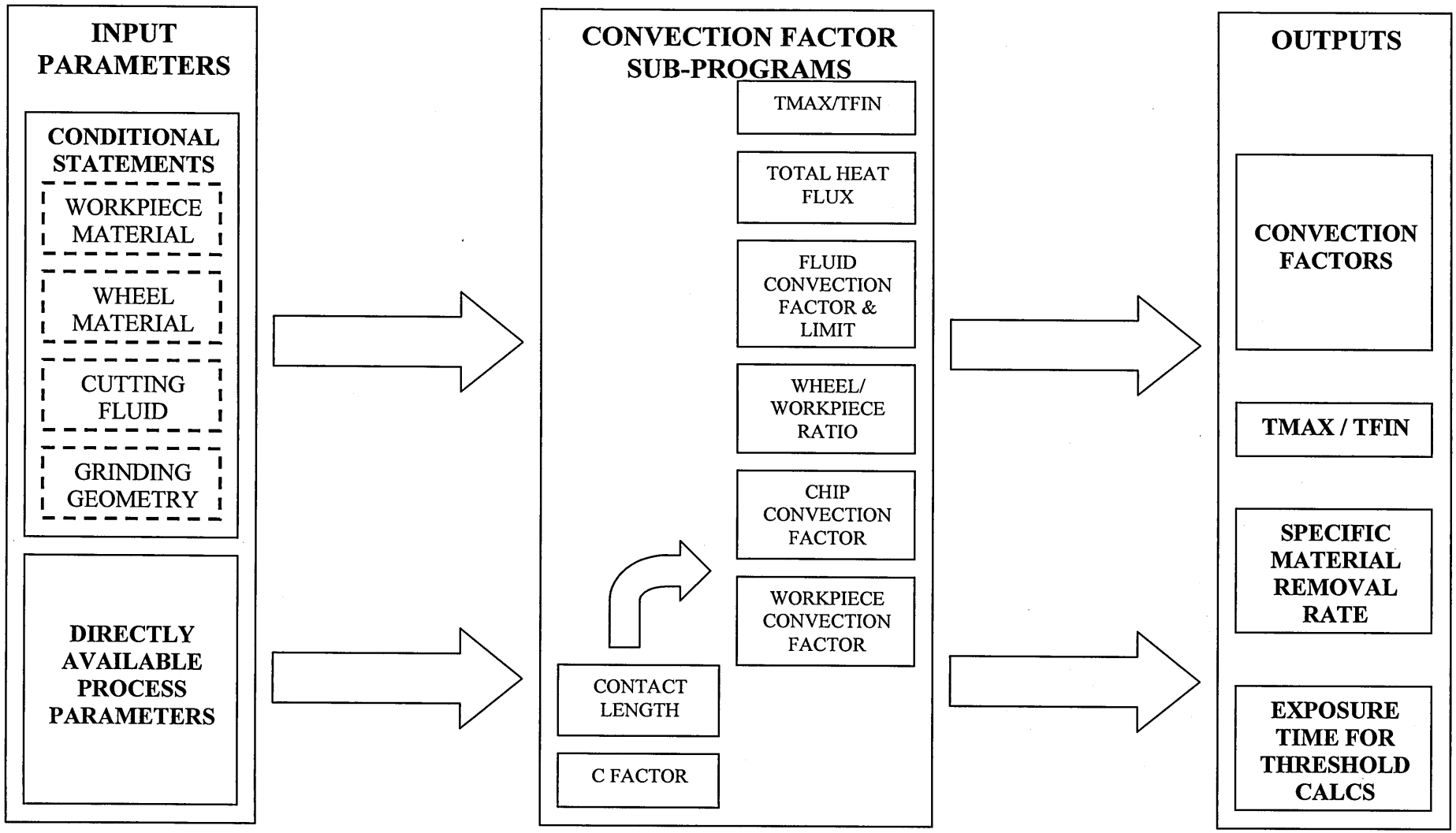

Figure 5.3: System Diagram of Pre Calculation for the Monitoring System.

5.2.1 Burn Thresholds

The thresholds are also calculated outside of the real time loop. These can be seen on the monitoring system diagram (figure 5.2) as pre calculate thresholds. A system diagram was presented in figure 4.3. However in this application more than one simple Boolean threshold is required to be more descriptive of the process. Hence the program sets lower limits, one 10% and the other 30% below the burn threshold. The 10% limit is intended to be used to warn the operator that the threshold is being approached and therefore allow corrective action to be taken. The 30% limit is used to determine whether the process is sub optimal or not: If both the estimated temperature and total heat flux are more than 30% of their respective thresholds the process is deemed to be sub optimal as the production rate can be increased safely. This is achieved using simple arithmetic operations and is represented on figure 5.2 by the "set lower limits" block.

5.2.3 Real Time Processes

The data acquisition must be performed in real time and output monitored power values to the main calculation loop. A buffer should be included so that data is not lost if the calculation procedure lags. This project does not consider the details of this part of the software as Lab View contains many automated features so that instrumentation can be controlled with little user input. In addition the existing monitoring system developed by Cranfield University has proven software that can perform this task. Each power value is then evaluated cyclically by the main process loop.

The first operation to be performed is to subtract the "spark out" power from the monitored power and calculate the total heat flux using equation 2.10. The finished workpiece temperature can also be calculated using the same sub program as discussed in section 4.3.3.

The total heat flux and finished workpiece temperature are now available to be evaluated against their respective thresholds. This is performed by using a series of conditional statements to compare the current values against the actual thresholds and

the 10 and 30% limits. These conditional statements control the text indicators, traffic lights and alarms discussed in section 5.1.

An agreement between the two indicators is also checked in the program by calculating each indicator's proximity to the burn threshold as a fraction of the threshold itself. If the difference in this fraction is greater than 30% the user is warned via the text output shown on the HMI in section 5.1.

5.3 Adaptive Control

As has already been stated in the previous sections, the monitoring system could be used as part of a constraint limited adaptive control system, the constraint being the burn limit of the grinding process. The monitoring system is able to provide feedback on the state of the process and it's proximity to the constraint so that the control can take corrective action.

This corrective action could be as simple as using the feed hold on the control system to stop the process and allow time for the operator to intervene. A more advanced approach would be to evaluate whether the process is operating in the creep feed or HEDG regimes and use the "feed rate override" to adjust the workpiece speed accordingly. If operating under HEDG conditions this would mean increasing the workpiece speed to increase the amount of energy expelled with the grinding chips. Conversely operating under creep feed conditions would require the workpiece speed to be slowed to reduce the energy input into the process as the material removal rate is not significant enough.

This would mean that some of the functionality of the parameter selection system would be required to evaluate whether the process is in the creep feed or HEDG regime. This could be performed by plotting temperature curves against specific material removal rate for constant cut depth and variable workpiece speed. If the gradient of the temperature with the specific material removal rate at the current workpiece speed is positive the process is operating in the creep feed regime. If it is negative it is in the HEDG regime.

Further discussion and development of this functionality is beyond the scope of this project. However this principle should form a good basis for further work.

5.3.1 Time to Burn Analysis

A further modification which maybe advantageous if an adaptive control system was to be developed would be a "time to burn" analysis.

The system design detailed in the previous sections uses a Boolean comparison to test whether either burn indicator is within 10% of the burn threshold, in order to allow corrective action to be taken. This approach is adequate for the intended monitoring function but does not take account the length of time required to take corrective action and the likely time between the warning and the onset of burn.

The time necessary to take corrective action is likely to be the time constant of the servo drive controlling the worktable, (i.e the time it takes to decelerate or accelerate) plus the maximum time between the control processor's checks of the status of the "feed rate override". This information is readily obtainable from control system manuals. It is more difficult to determine how long it will take for burn to be realised if there is a transient in the process which is causing the workpiece temperature to increase. An example of such a transient is fluid film burn out.

Lab View has functions that can fit a spline curve to previous data and extrapolate this curve to a given point. A possible approach would be to perform this fit on calculated temperatures and total heat fluxes against time and extrapolate the curve by the minimum time to perform corrective action (plus a safety factor) and then evaluate the process against the thresholds at this point. This provides us with greater assurance that burn can actually be avoided. An example system diagram is shown in figure 5.4.

The spline extrapolation has the advantage of being extremely fast to execute and provides a good approximation to all functions, as stated by the Lab View 7.1 documentation.

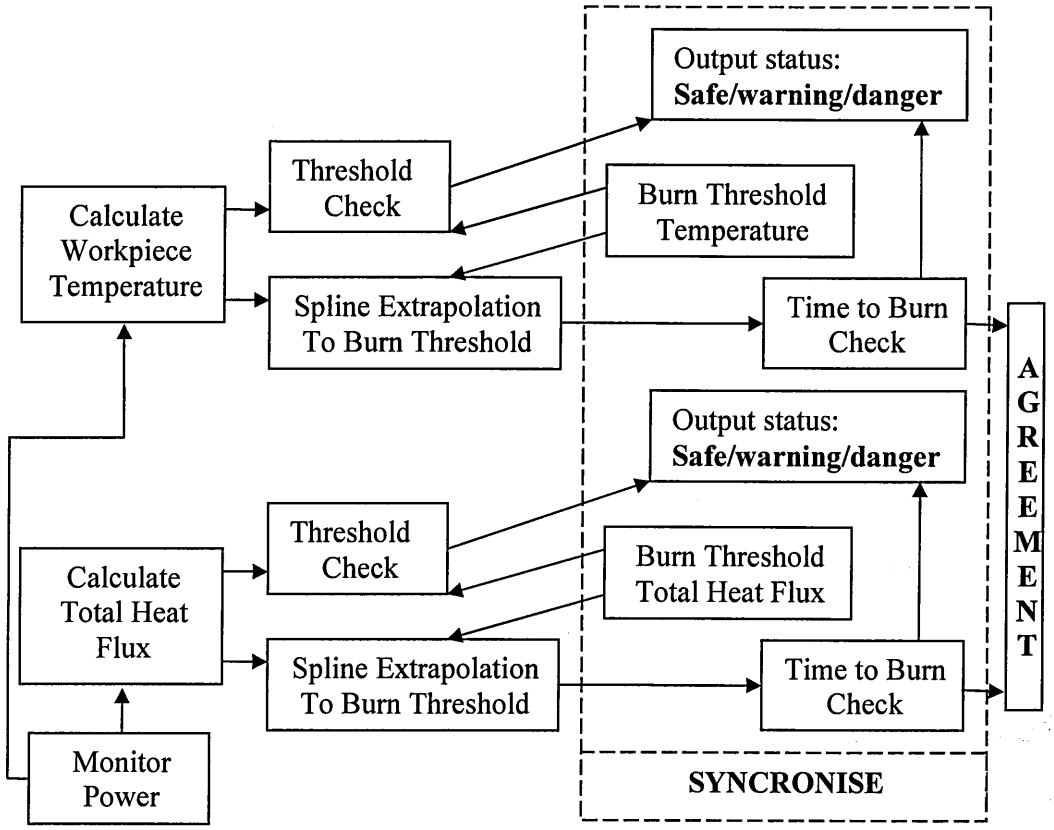

Figure 5.4: Time to Burn Analysis System Diagram

Again an implementation of this strategy is beyond the scope of this study and represents a direction for further work.

CHAPTER 6: DEMONSTRATION OF SYSTEM CAPABILITY

In this chapter the relevance of the system to industry is demonstrated in terms of its application to process design and control.

6.1 Process Design Example

If we take a hypothetical process planning situation where a planar component made of 51CrV4 has to be surface ground removing 3mm of stock material. The wheel, wheel speed and grinding fluid shall be considered to be predetermined by company policy; a 200 x 20 CBN wheel running at 146m/s and oil based fluid. These restrictions are common for production engineers in aerospace where processes must be accredited. Since there is 3mm of stock it would be sensible to choose this depth of cut as it well within the capabilities of a grinding machine intended for HEDG. A constant cut depth should then be specified in the optimisation options in order to observe the effect of varying workpiece speed. It will also be assumed that the maximum workpiece speed the machine is capable of is 0.15m/s.

These parameters were then put into the parameter selection system and the program run. The results can be seen in figures 6.1 and 6.2 Figure 6.1 is shown only to demonstrate that the user is warned that the valid range for the heat has been exceeded and so should not be taken into account in this instance.

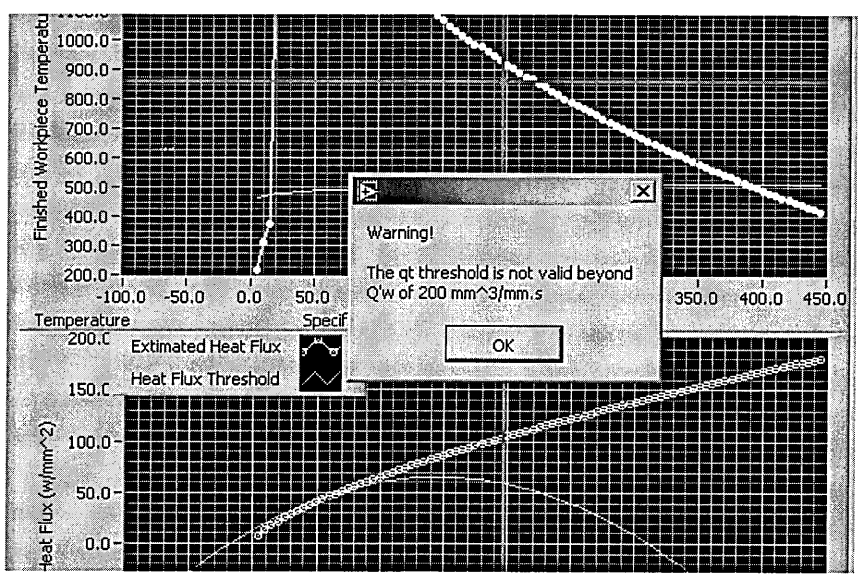

Figure 6.1: Demonstration of Heat Flux Range Warning.

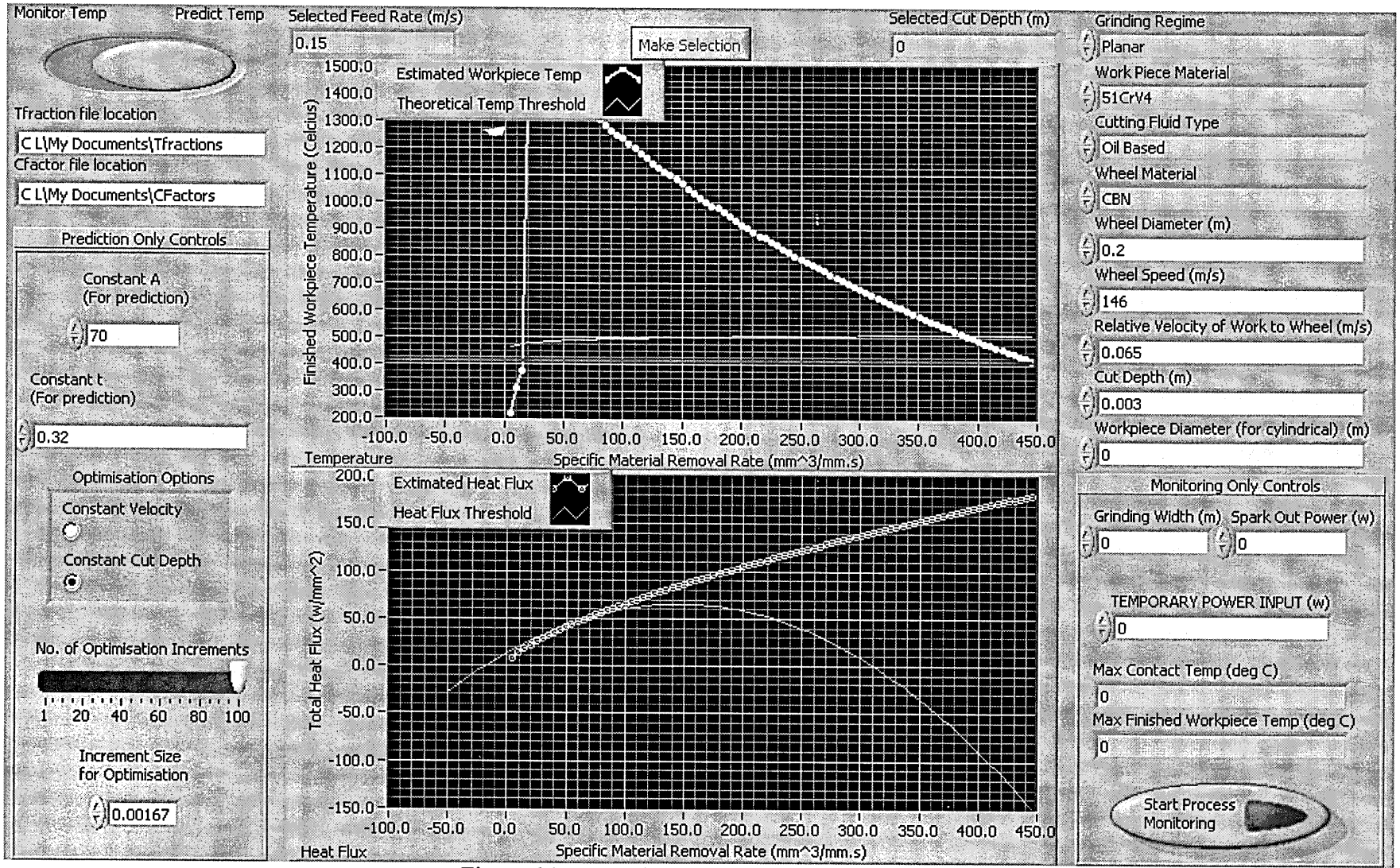

Figure 6.2: Example Parameter Selection Results.

6.1.1 Discussion of Process Design Results

The screen shot in figure 6.2 shows the finished workpiece temperature (in green with white points)against and the theoretical threshold (in yellow) against specific material removal rate. The characteristic variation in temperature can be seen with a steady increase until fluid burn out is reached causing a massive increase that exceeds the burn threshold temperature. Following this the temperature gradually reduces as the effect of heat lost to the grinding chip becomes more significant until eventually bringing it below the burn threshold once more.

Therefore there are two ranges of specific material removal rates that are estimated not to result in burn one being typical of a creep feed process and the other of a HEDG process. The highest workpiece speed possible in the creep feed regime is 0.05m/s. The blue cursor is shown selecting the optimum HEDG condition (i.e the greatest material removal rate), which is actually the maximum possible workpiece speed of 0.15m/s.

Selecting this HEDG condition would increase the production rate by three times over the creep feed condition and the system allows the production engineer to see this. It is quite feasible that an even more conservative workpiece speed maybe chosen in a real situation without the use of such a process planning aid. It may also that several conditions resulting in burn are selected before a safe one is found, which is expensive and time consuming.

The system also has the advantage of increasing the production engineers understanding of the process, as they are unlikely to have time to learn all of the theory behind thermal process design in grinding. The user can see the trends with material removal rates and also the effects of different wheel types and speeds.

6.2 Process Monitoring Example

For this example the same process conditions as in section 6.1 will be used but the workpiece speed that represents a creep feed process (0.05m/s) will be selected so that both the temperature and heat flux thresholds are both valid for demonstration purposes. Process monitoring can then be simulated by manually inputting a value for the grinding power. The example in figure 6.3 shows the system using the ideal power. As the process was correctly designed using the parameter selection system, safe grinding conditions are indicated by text, the green lights and the absence of any alarms. The agreement status of the two indicators are also shown to be acceptable.

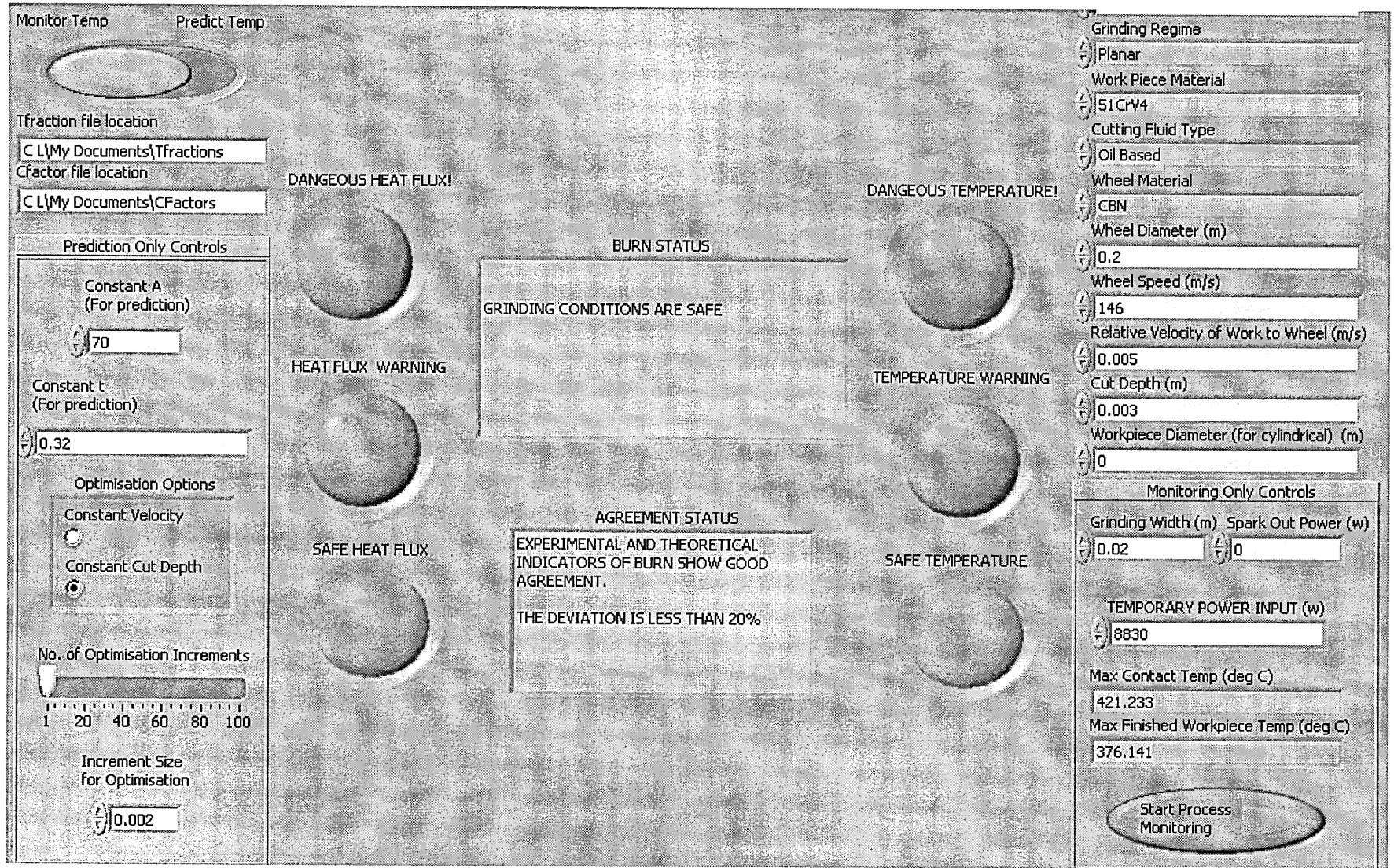

Figure 6.3: Example Process Monitoring; Safe Conditions.

6.2.1 Simulated Wheel Wear

Malkin (1989) states that as a grinding wheel wears the net grinding power increases, this may cause burn of the workpiece as the energy input to the process has increased but the ability of the various heat sinks to dissipate it, has not. This situation is therefore simple to simulate by increasing the power input to the system beyond the ideal model. This simulation is shown in the screen shot of the monitoring system in figure 6.4.

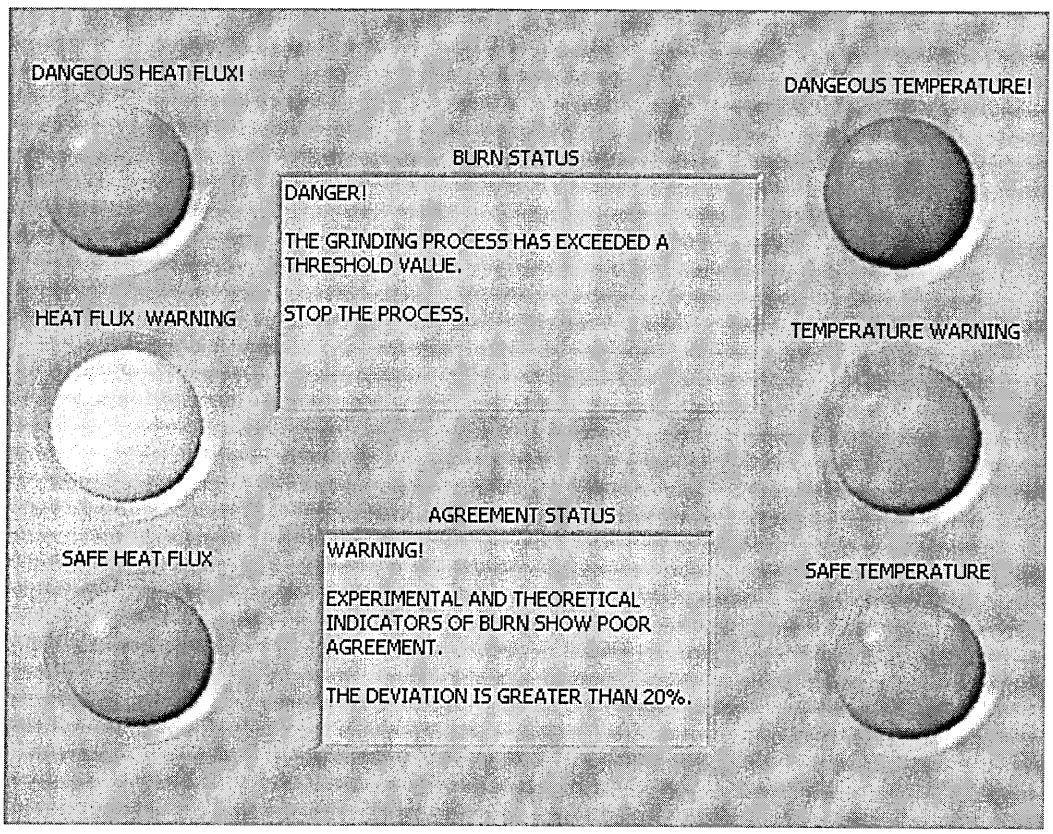

Figure 6.4: Example Process Monitoring; Simulated Wheel Wear.

Increasing the power by 15% to simulate wheel wear causes the heat flux threshold to issue a warning that it is close to the threshold and the temperature to indicate danger as the threshold has been exceeded. Since the system is set up to maximise safety, exceeding just the one threshold causes the burn status to recommend stopping the process and an alarm is sounded. The agreement status is now greater than 20%

deviation this is because fluid burn out has been reached causing a large discontinuity in temperature.

This would enable the operator to take action and possibly prevent damage occurring to the component. It is also important to consider that if such a system was not used the wheel wear and resulting damage may not be detected until several components have been damaged. This is because as Malkin (1989) suggests the visible signs of burn (temper colours) are often removed by "spark out" (a final pass to clean up the surface with no further in feed.) This represents a worse situation than simply scrapping a component as it may mean that these components with compromised surface integrity could fail prematurely in service, with far greater financial implications.

6.3.2 Simulated Sub-Optimal Conditions

Another function of the system is to notify the user when the machine is being seriously under utilised and the burn indicators are both detected to be below 30% of their thresholds. Take the previous process conditions but with a reduced workpiece speed of 0.003m/s and using the associated ideal power. The resulting status is shown in figure 6.5.

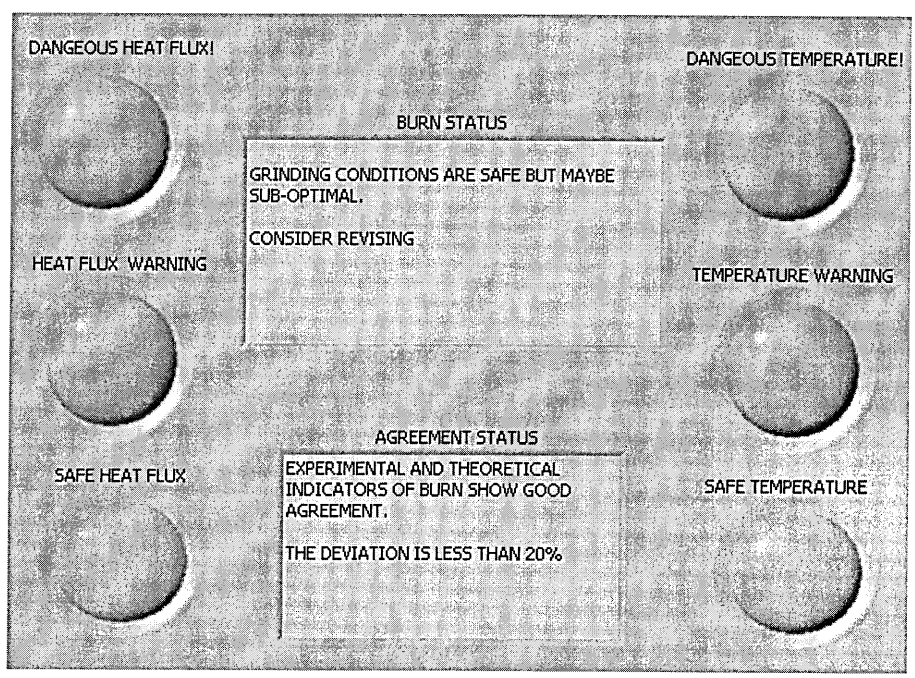

Figure 6.5 Example Process Monitoring; Sub Optimal Conditions.

Figure 6.5 shows the user interface displaying safe conditions with good agreement. However the burn status indicates that the process conditions maybe sub optimal to encourage these to be revised using the parameter selection system. This feature is important to ensure that any culture of conservatism within a company does not restrict the production rates that can be safely achieved and reinforces the application of the parameter selection system.

6.3 Finished Workpiece Temperature as a Control Parameter

Whilst performing these simulations, a characteristic of the finished workpiece temperature was highlighted that brings into question it's effectiveness as a control parameter.

As discussed in section 2.3.5 the transition grinding fluids transition from nucleate to film boiling reduces the convection coefficient to zero. This results in a huge increase in finished workpiece temperature. Experimentation demonstrated that the change in net grinding power necessary to bring about this transition was incredibly small; this can be observed from figure 6.6.

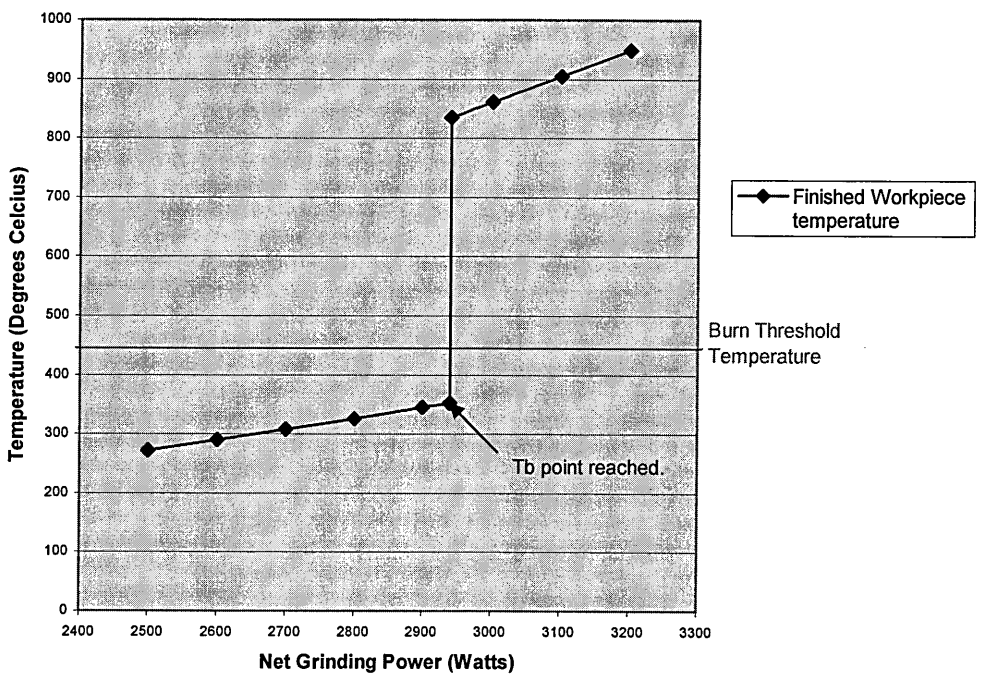

Figure: 6.6: Temperature vs. Increasing Power with Constant Process Parameters.

Figure 6.6 was created by simulating a grinding process that was under going significant wheel wear, i.e. gradually increasing the net power input for the process whilst other process parameters were held constant.

As the power was increased the total heat flux approached the empirical threshold and so the system activated the amber warning light and indicated that the heat flux was now within 10% of the burn threshold. Conversely, the finished workpiece temperature continued to indicate a safe condition as it was more than 10% below the burn threshold temperature.

This continued until the film boiling transition temperature was reached and the finished workpiece temperature increased by approximately 500°C, which is significantly greater than the burn threshold temperature. At this point both the heat flux and temperature register dangerous conditions and alert the user with an alarm.

As stated the change in power to move through this transition is very small; in this test a difference of 0.1 nano watts was found to be sufficient. This is restricted by the resolution of the power input variable and so the real increment is likely to be smaller in reality.

6.3.1 Discussion of Workpiece Temperature as a Control Parameter

It has been demonstrated that a change in the monitored net power of less than 0.1 nano watts could result in a temperature difference of approximately 500°C and cause burn to occur.

In one sense it validates the effectiveness of using a multi parameter monitoring approach as despite the failing of one parameter the total heat flux still warns of the close proximity to the burn threshold.

However, it is clear that if such a minute change in power can produce such a massive nonlinearity in temperature, moving it past the burn threshold without warning, it cannot be used effectively to prevent the onset of burn. It can only serve to notify the

machine operator that burn has occurred in a monitoring function and would not enable the operator or a control system to take corrective action.

This does not necessarily mean that attempting to control workpiece temperature in an adaptive control system is not feasible although it does bring into question the use of the finished workpiece burn temperature as a threshold. It may be more effective to use the film boiling transition temperature itself as the threshold, which is related to the maximum contact temperature. The huge temperature increase at the transition commonly results in burn, and so the threshold can be used to pre-empt its occurrence. The relationship between the film boiling transition and burn was noted by Jin and Stephenson (2002).

The use of a threshold based on the finished workpiece temperature is still valid for parameter selection as this ultimately determines whether burn occurs or not and there is no dynamic element to consider.

CHAPTER 7: SYSTEM VALIDATION

To validate the system it is necessary to make comparisons between grinding temperatures estimated by the software and measured temperatures from real grinding tests. It is also important to verify whether burn has actually occurred when the monitoring system indicates that it has.

Due to the time constraints of the project it was not possible to perform online grinding trials. As an alternative, historical data was used to simulate real grinding conditions.

7.1 Embedded Thermocouple Measurement Comparison

Rowe and Jin (2001 c) conducted experiments on a 6 kW surface grinder using an alumina wheel. Workpieces consisted of two slices of AISI 1095 steel sandwiching a constantan wire to form a J type thermocouple and so a direct measurement of the maximum contact temperature could be made. The net spindle power was recorded during the test.

It is a simple matter to input the process parameters into the parameter selection system and calculate temperatures for comparison that are based on the ideal specific energy curve for the process. However, a modification has to be made so that the maximum contact temperature is output instead of the finished workpiece temperature that is of interest for process design.

This can therefore be used to compare maximum contact temperatures estimated from the monitoring system with the thermocouple results. The program was modified to accept a single power input instead of receiving an array of power values from the instrumentation.

Test Conditions	
Wheel Material: Alumina	Workpiece Material: AISI 1095
Wheel Speed: 55m/s	Workpiece Speed: 0.2 – 0.32m/s
Depth of Cut: 0.4 – 1mm	Coolant type: Water Based Emulsion

Table 7.1: Thermocouple Test Conditions, Rowe and Jin (2001 c).

Test	1	2	3	4
Specific Material Removal Rate ($mm^3/mm.s$)	81	196	230	288
Measured Specific Power (kW/mm)	1.39	2.61	3	3.17
Measured Temperature (°C)	1250	1350	1050	180

Table 7.2: Results from Thermocouple Tests, Rowe and Jin (2001 c).

Tales 7.1 and 7.2 were used to generate estimated temperatures for comparison. A value for the exponent t used in the prediction of the ideal specific energy (equation 2.11) was estimated to be 0.32. The specific chip energy was taken to be the limiting chip energy (i.e the energy required to bring the material close to melting point, 8.1 J/mm^3.) as suggested by Rowe and Jin (2001 c). The results can be seen in figure 7.1.

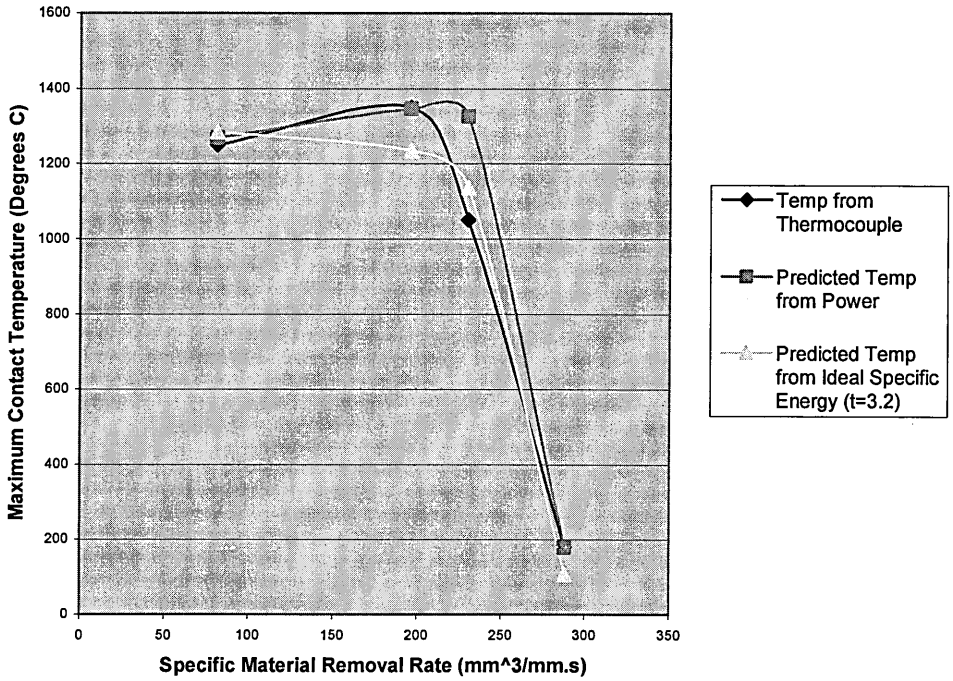

Figure 7.1: Thermocouple Measured and Estimated Maximum Contact Temperatures.

7.1.1 Embedded Thermocouple Comparison Discussion

Figure 7.1 shows good correlation between measured and both sets of estimated temperatures.

However after the first test the temperature estimated from the ideal specific energy under estimates the temperature by approximately 8%. Since the prediction based on measured power produces a much more accurate result, it is due to a deviation from the ideal specific energy curve. This deviation is likely to be due to wheel wear, Malkin (1989) states that wheel wear and the development of wear flats increases the net grinding power (and therefore specific energy) considerably. Alumina wheels are not well suited to HEDG conditions and do wear quite dramatically when subjected to high material removal rates.

The effect of the high specific material removal rates employed in HEDG can clearly be seen from figure 7.1. Beyond a certain specific material removal rate, enough energy is removed by the chip to bring the temperature below the film boiling

transition and into nucleate boiling. The coolant is then active in removing heat energy and a massive drop in contact temperature results.

7.2 PVD Coating Melt Depth Measurement Comparison

Walton (2005) used a PVD coated workpiece to measure the maximum contact temperature during grinding. Low melting point coatings of Indium, Bismuth Antimony or Zinc are applied too notches cut into the workpiece in 200nm layers. The high temperatures produced by the grinding process melted the coatings and the resulting melt depth can be analysed to calculate the maximum contact temperature. Walton (2005) and Kato (2000) found this method to produce reliable results.

Tests were performed using conditions ranging from creep feed to HEDG on an Edgetek surface grinding machine that is capable of grinding under the the HEDG regime.

Test Conditions	
Wheel Material: CBN	Workpiece Material: 51CrV4
Wheel Speed: 146m/s	Workpiece Speed: 0.00125 – 0.125m/s
Depth of Cut: 4 – 8mm	Coolant type: Oil Based
Grinding Width: 2 – 4mm	Specific Material Removal Rate: 5-1000mm^3/mm.s

Table 7.3: PVD Test Conditions, Walton (2005).

Test	**1**	**2**	**3**
Specific Material Removal Rate (mm^3/mm.s)	5	500	1000
Measured Power (kW)	1.15	20.12	19.67
Measured Temperature (°C)	285	927	1082

Table 7.4: Results from PVD Tests, Walton (2005).

Tables 7.3 and 7.4 were used to generate estimated temperatures for comparison. A value for the exponent t used in the prediction of the ideal specific energy (equation

2.11) was estimated to be 0.31 for this process. A specific chip energy of 6 J/mm^3 estimated and was found to provide good results in this instance, which corresponds to a chip temperature of around 1200°C. The results can be seen in figure 7.2.

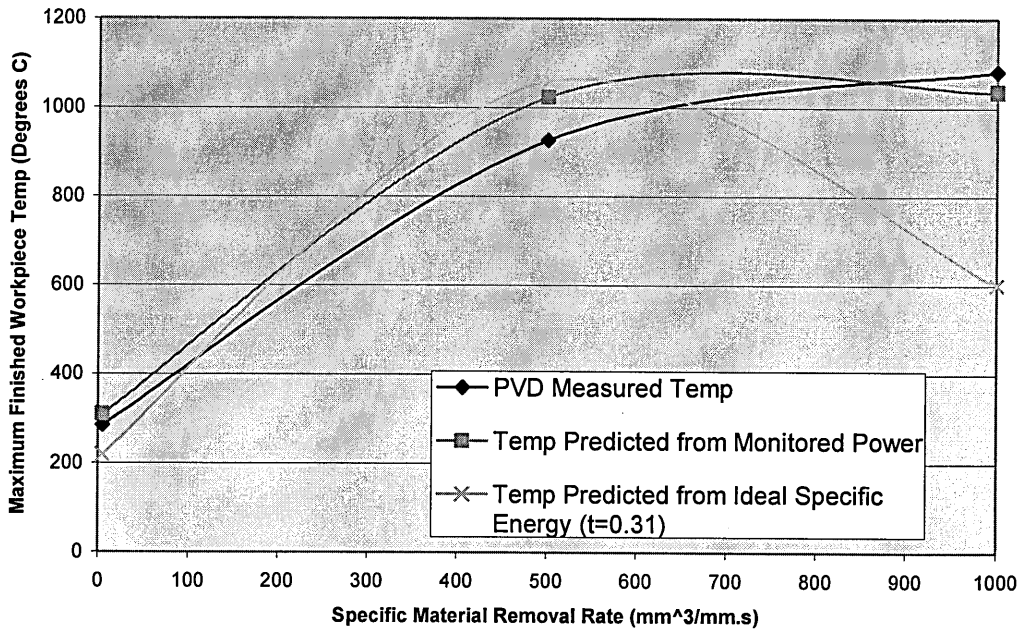

Figure 7.2: Comparison of Maximum Contact Temperatures Calculated from PVD Melt Depth with Estimated Temperatures.

7.2.1 PVD Coating Melt Depth Measurement Comparison Discussion

The PVD measured temperature and the temperature prediction based on the monitored power show good correlation throughout the range of specific material rates. The temperature prediction based on the ideal specific energy provides a good estimation of the first two tests but drastically underestimates the temperature for the last test. It is possible that wheel wear has occurred at this point causing the specific energy of the process to be greater than that predicted by the ideal specific energy curve.

Despite this discrepancy the estimated temperature is still well above the burn threshold. The parameter selection system would therefore prevent this condition from being chosen and so is still performing its function adequately.

7.3 Online Burn Prediction Simulation

Grinding tests performed by Dr Jin of Cranfield University involved a metallurgical study of the ground workpieces, to determine whether burn had occurred. This involves cutting and polishing samples of the workpieces and examining under a microscope for a dark layer of OTM or a white layer UTM as described in section 2.4.

The power was monitored during the tests and the same process parameters and grinding machine as the PVD melt depth measurement tests were used. There is also an additional test performed with a specific material removal rate of $50mm^3/mm.s$ The recommendations of the monitoring system can therefore be compared with the results of this metallurgical study as can be seen in table 7.5.

S. M. R. R. ($mm^3/mm.s$)	Metallurgical Study Results	Monitoring System Recommendations
5	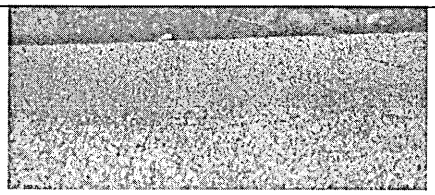 A 35 micron layer of OTM can be seen suggesting burn has occurred.	Heat flux threshold exceeded but temperature threshold is not approached. (Hence the observed OTM may actually be a staining effect occurring after etching.)
50	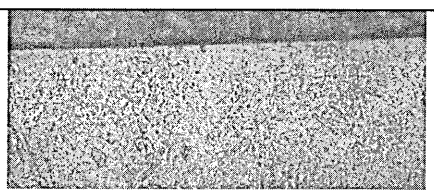 No damage.	Safe Conditions
500	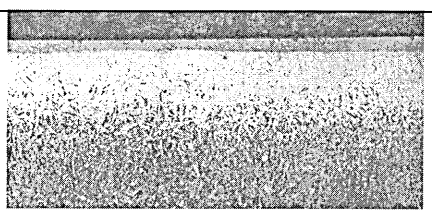 Serious damage has occurred with 50 micron deep white UTM layer.	Heat flux and temperature thresholds exceeded. (The system also indicated that the heat flux threshold was outside its valid range.)
1000	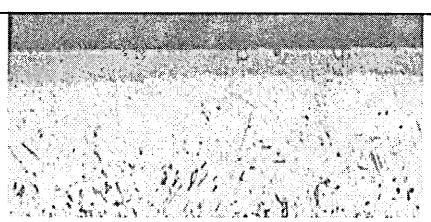 Serious damage has occurred with an even deeper white UTM layer.	Heat flux and temperature thresholds exceeded. (The system also indicated that the heat flux threshold was outside its valid range.)

Table 7.5: Comparison of Monitoring System Burn Predictions with Observed Metallurgical Transformations.

7.3.1 Discussion of Simulated Online Burn Prediction Results

The monitoring system shows excellent agreement with the metallurgical results. These results also demonstrate the efficacy of the use of the two threshold approach. The $5mm^3/mm.s$ specific material removal rate test resulted in mild damage to the workpiece. This was not indicated by the theoretical temperature burn threshold but was by the empirical heat flux threshold and so the operator would still receive the correct information about the state of the process.

CHAPTER 8: CONCLUSION

The following text will briefly conclude the findings of this work:

1) Literature suggests that grinding is an expensive and complex process that has much to gain from the use of tools to select and maintain optimal process conditions. (Chapter 2)
2) Literature suggests that greatest restriction on higher production rates is the risk of thermal damage to the workpiece, which may compromise the integrity of the finished component. (Chapter 2)
3) Literature suggests that the development of HEDG provides an opportunity to increase production rates whilst maintaining low finished workpiece temperatures. Although it increases the need for process design and monitoring tools as it challenges much of the conventional wisdom in grinding. (Chapter 2 and Chapter 6)
4) Literature suggests that the thermal models developed by Rowe, Jin and Stephenson provide a means of reliably estimating finished workpiece temperatures. (Chapter 2)
5) Literature suggests that the most significant type of thermal damage for steels is burn and so the system is aimed specifically to address this problem. (Chapter 2)
6) The majority of existing predictive and reactionary systems for parameter selection and process monitoring rely on empirically derived rule bases. Empirically derived indicators of burn maybe highly effective within a limited range but can produce erroneous results outside of that range. As noted from work by Ali (2003) which fails to take account of HEDG conditions. (Chapter 3)
7) Those existing systems that rely on analytical methods often use models that are not applicable to HEDG. (Chapter 3)
8) The existing system developed by Cranfield University uses an analytical model applicable to HEDG but lacks the speed to be used in online thermal monitoring and also to be developed into an effective parameter selection system. (Chapter 3)

9) The ideal solution would therefore incorporate the advantages of both empirical and analytical methods in one system and utilise all possible means to minimise processing time. (Chapter 3)

10) Work at Cranfield University has presented the total heat flux as a viable empirical burn threshold generated from measured net grinding power and this fulfils the. (Chapter 3)

11) The temperature threshold proposed by Jin (2005 b) is unique in its use of a tempering parameter to take account of the time dependency of burn, which becomes significant in HEDG. Hence this should be employed in the new system. (Chapter 3)

12) The merits of using Lab View have been established along with the best practice software design method for this application. (Chapter 3)

13) A user interface has been developed that should enable a production engineer to select optimal grinding conditions and provide a greater understanding of the thermal aspects of grinding, particularly with reference to HEDG. (Chapter 4)

14) The estimation of C factors and Tfin/Tcon has been identified as the major restriction on the overall temperature calculation time. (Chapter 4)

15) The estimation of C factors and Tfin/Tcon using "look up tables" and linear interpolation has been demonstrated to drastically reduce this calculation time, whilst introducing a mean error of 0.18%. (Chapter 4)

16) The use of equation 2.17 allows the user to input an estimated chip energy and has been established to provide flexibility without the time penalty of alternatives. (Chapter 4)

17) A user interface that provides operators with simple information about the state of the process has been developed. (Chapter 5)

18) A strategy for the prediction of grinding burn has been developed. (Chapter 5)

19) The potential for developing the monitoring system into an adaptive controller has been reviewed and directions for further work established. (Chapter 5)

20) The discontinuity in finished work piece temperature at the nucleate to film boiling transition makes the burn threshold temperature a poor control constraint for an adaptive controller. (Chapter 6)

21) The film boiling transition itself has been demonstrated to be a more effective control constraint. (Chapter 6)

22) The potential of the parameter selection system to reduce cycle times by optimal thermal process design has been demonstrated. (Chapter 6)
23) The potential for the monitoring system to reduce the occurrence of thermal damage and therefore scrap has also been demonstrated. (Chapter 6)
24) The temperature estimation of the parameter selection and monitoring systems has been shown to provide good agreement with measured grinding temperatures using the embedded thermocouple and PVD melt depth methods. (Chapter 7)
25) Preliminary simulations have demonstrated that the monitoring system can predict the occurrence of burn. (Chapter 7)

8.1 Suggested Further Work

The most of important area for further work is to extend the validation beyond simulation from previous experimental data to genuine machine trials. This should involve the use of the parameter selection system to select a range of grinding conditions from shallow cut to HEDG that are just below and just above the burn threshold. Test pieces should then be ground using these parameters and the output of the monitoring system should be noted. The predictions of both systems can then be compared with a metallurgical study of the test pieces to determine whether burn occurred or not.

It is suggested in section 6.4., that the nonlinearity of the finished workpiece temperature, at the film boiling transition, means that a temperature based burn threshold is ineffective for process monitoring. The film boiling transition temperature itself, was identified as a more reliable alternative and so the monitoring system should be modified to suit.

Another area for further work would be to develop the monitoring system into an adaptive controller taking forwards the concepts presented in section 5.3. The Lab View environment could still be used as control algorithms from classical to fuzzy logic are available within the package and its continued use would avoid compatibility issues.

REFERENCES

Aguiar, P. R. (1997). *"Burn Monitoring in Grinding Process by utilizing the Acoustic Emission and Electric Power Signals."* Doctorate thesis, Escola Politacnicada USP.

Ali, Y. M., Zhang, L. C. **(2003).** *"A Fuzzy Model for Predicting Burns in Surface Grinding of Steel."* International Journal of Machine Tools and Manufacture Vol. 44, pg. 563-571.

Dotto, F. R. L., Aguiar, P. R., Bianchi, E. C. **(2002).** *"In Process Thermal Damage Detection in Grinding with Monitoring via Internet."* Seventh International Conference on Control, Automation, Robotics and Vision, Singapore.

Field, M. Kahles, J. F, **(1971).** *"Review of Surface Integrity of Machined Components"*. Annals of CIRP Vol 20/1, pg. 153-163.

Gibbons, A. (2005). *"Applications of Viper Grinding Technology."* Advances in Grinding Technology, IGT Annual Seminar.

Hahn, R. S., (1962). *"On the nature of the grinding process."* Proceedings of the 3rd International Machine Tool Design and Research Conference, Birmingham pg. 129-154.

Hiroshi Eda, Kozo Kishi Nobuyuki Usui, Hideo Veno, Yoshiaki Kakino and Akihiko Fujiwara, Bull. **(1984).** Japanese Society of Precision Engineers, Vol. 18/4 pg. 299–304.

Huang Ren, Shi Xiurong, Ding Ruilian, Zhong Binglin, Mao Yuliang, J.A. Brandon. **(1992)** International Journal of Machine Tools and Manufacture, Vol. 32/16 pg. 767–779.

Johnstone, I. (2002) *"A Critical Study of High Efficiency Deep Grinding."* PhD Thesis, Cranfield University.

Jin, T., Stephenson, D. J., Corbett, J., **(2002).** *"Burn threshold of high carbon steel in high efficiency deep grinding"* Proceedings of the Institution of Mechanical Engineers, Part B, Journal of Engineering Manufacture, Vol. 216, pg. 357-364.

Jin, T., Stephenson, D. J., Rowe, W. B. **(2003).** *"Estimation of the Convection Heat Transfer Coefficient of Coolant within the Grinding Zone."* Proceedings of the Institution of Mechanical Engineers, Part B, J of Engineering Manufacture, Vol.217, pg. 397-407.

Jin, T., Stephenson, D. J., **(2005 a).** *"Analysis of Grinding Chip Temperature and Energy Partitioning in High Efficiency Deep Grinding"* Submitted to the Proceedings of the Institution of Mechanical Engineers, Part B, J of Engineering Manufacture.

Jin, T., Stephenson, D. J., **(2005 b).** *"Analysis of the Depth of Workpiece Sub-Surface Damage in Creep Feed and High Efficiency Deep Grinding"* Submitted to the Proceedings of the Institution of Mechanical Engineers, Part B, J of Engineering Manufacture.

Jin, T., Walton, I., (2005 c). Private communication with members of academic staff from Cranfield University, UK.

Kato, T., Fuji, H. **(2000).** *"Temperature Measurement of Workpieces in Conventional Surface Grinding."* Journal of Manufacturing Science and Engineering, Vol. 122, pg. 297-303.

Kodácsy, J., Szabó, A. **(2000).** *"A New Temperature Measuring System in Grinding."* Seminar "Moderne Schleiftechnologie" Villingen-Schwenningen Germany.

Koenig, W. (1991) *"Artificial Intelligence and Simulation in Grinding Processes."* 11th European Congress on Operational Research, Acahen.

Loewen, E. G., Shaw, M. C., (1954). *"On the Analysis of Cutting Tool Temperature"*. Transactions of the American Society of Manufacturing Engineers, Vol. 74, pg. 73-86.

Outwater, J. C., Shaw, M. C. **(1952).** *"Surface temperatures in grinding."* Transactions of the American Society of Manufacturing Engineers, Vol. 74, pg. 73-85.

McCormack, D. F., Rowe, W. B, Jin, T. **(2001)** *"Controlling Surface Integrity of Ground Components with CBN."* 4th International Machining and Grinding Conference, Troy, Michigan USA, Society of Manufacturing Engineers Technical Paper MR01-236. pg. 1-13.

Malkin, S. (1989). *"Grinding Technology – Theory and Applications of Machining with Abrasives."* Ellis Horwood Limited, Chichester.

Marinescu, I. B., Rowe W.B., Dimitrov B., Inasaki, I. **(2004).** *"Tribology of Abrasive Machining Processes"*. William Andrew, Inc. USA.

Midha, P. S., Zhu, C. B., Trmal, G. J. **(1991).** *"Optimum Selection of Grinding Parameters Using Process Modelling and Knowledge Based System Approach"* Journal of Materials Processing Technology, Vol. 28 pg. 189-198.

Rowe W.B., Bell, W.F., Brough, D. **(1986).** *"Optimisation Studies in High Material Removal Rate Centreless Grinding."* Annals of the CIRP Vol. 35/1, pg. 235-238.

Rowe, W.B., Pettit, J.A., Boyle, A., Moruzzi, J. L. **(1988).** *"Avoidance of Thermal Damage in Grinding and Predicition of Damage Threshold."* Annals of the CIRP Vol. 37/1, pg. 327-330.

Rowe, W.B., Morgan, M.N., Pettit, J.A. **(1990).** *"A Discussion of Thermal Models in Grinding."* Society of Manufacturing Engineers, Paper no. MR90-516

Rowe, W.B., (2001 a). *"Thermal Analysis of High Efficiency Deep Grinding."*

International Journal of Machine Tools & Manufacture, Vol. 41, pg. 1-19.

Rowe, W.B., (2001 b). *"Temperature Case Studies in Grinding including an Inclined Heat Source Model."* Proceedings of the Institution of Mechanical Engineers, Vol. 215, pg. 473-491.

Rowe, W.B., Jin, T., **(2001 c).** *"Temperatures in High Efficiency Deep Grinding."* Annals of CIRP, Vol. 50(1), pg. 205-208.

Shaw, M. C. (1996). *"Principles of Abrasive Processing."* Oxford Science Publications, New York.

Snoeys, R., Maris, M. and Peters, J., **(1978).** *"Thermally Induced Damage in Grinding"*, Annals of the CIRP, Vol 27/2, pg. 571.

Stephenson D.J., Laine E, Johnstone I, Baldwin A, Corbett J., **(2001).** *"Burn Threshold Studies for Superabrasive Grinding Using Electroplated CBN Wheels."* Proc 4th International Machining & Grinding Conference USA 7-9 May 2001, SME Technical Paper MR01-219.

Stephenson D.J., T. Jin. **(2003).** *"Physical Basics in Grinding."* 1st European Conference on Grinding, Aachen, Germany. K. Werner, P. Klocke, E. Brinksmerer (Eds.), Fortsehr-Ber. VDI Reihe 2 Nr.643, VDI Verlag, pg. 301-1321.

Tawakoli, T. (1993). *"High efficiency deep grinding: technology, process, planning and economic application."* Mechanical engineering publications.

Tang, J.S. , Pu, X.F., Xu, H.J., Zhang, Y.Z. **(1980).** Annuals of CIRP Vol. 39/1 pg. 353–356.

Travis, J. (2001) *"Lab View for Everyone."* Second Edition. Prentice Hall PTR.

Trmal, G. J., Zhu, C. B., Midha, P. S. **(1992).** *"An Expert System for Grinding Process Optimisation"* Journal of Materials Processing, Vol. 33 pg. 507-517.

Walton, I. M., Stephenson, D. J., and A. Baldwin. **(2005)** *"The Measurement of Grinding Temperatures at High Specific Material Removal Rates."* Submitted to the International Journal of Machine Tools & Manufacture.

Woodbury, R. S. (1959). *"History of the Grinding Machine."* 1st Edition. MIT Press, Cambridge MA.